ON THE LIMITS TO PRECISION IN SPECTROSCOPY

WILLIAM H. WING

PHYSICS DEPARTMENT, OPTICAL SCIENCES CENTER,
AND ARIZONA RESEARCH LABORATORIES
UNIVERSITY OF ARIZONA, TUCSON, ARIZONA 85721 U.S.A.

in

Proceedings of the 1983 International School and Symposium on Precision Measurement and Gravity Experiment, Taipei, Republic of China, January 24 - February 2, 1983, ed. by W.-T. Ni (Published by National Tsing Hua University, Hsinchu, Taiwan, Republic of China, June, 1983)

ON THE LIMITS TO PRECISION IN SPECTROSCOPY

William H. Wing

Physics Department, Optical Sciences Center, and Arizona Research Laboratories
University of Arizona, Tucson, Arizona 85721 USA

Abstract: - Modern techniques of coherent high resolution spectroscopy, often involving laser sources, have developed the subject far beyond what it was in the great classical spectroscopic era which coincided with the origins and development of our present theories of atomic and molecular structure. Precision and sensitivity have increased so rapidly recently that it is appropriate to ask what physical barriers there are to indefinite progress, and to what extent they may be overcome. These questions are the central focus of this essay.

OUTLINE

I. THE PROGRAM OF HIGH RESOLUTION SPECTROSCOPY
II. CONVENTIONAL SPECTROSCOPY
III. UNCONVENTIONAL SPECTROSCOPY
IV. ELEMENTS OF ATOMIC STRUCTURE: THE HYDROGEN ATOM
V. ESTIMATES OF LINE BROADENING EFFECTS IN CONVENTIONAL SPECTROSCOPY
   A. Effects of atomic motion
   B. Stray quasistatic fields
   C. Rapidly varying stray fields
   D. Summary
VI. REDUCTION OF DOPPLER BROADENING
   A. Temperature reduction
   B. Mass increase
   C. Fast-beam kinematic compression
   D. Saturation spectroscopy
   E. Right-angle interaction
   F. Doppler-free multiphoton spectroscopy
VII. TRANSIT BROADENING
   A. Rabi resonance
   B. Separated oscillatory fields
VIII. ELIMINATION OF DOPPLER AND TRANSIT BROADENING BY CONFINEMENT OF PARTICLES
   A. The role of photon momentum
   B. Giving the photon momentum away: origins
   C. Example: the hydrogen storage-box maser
   D. Underlying principle of recoilless absorption
   E. Confined particle spectroscopy
IX. REDUCTION OF RADIATION BROADENING
X. SPECTROSCOPIC SOURCES AND INSTRUMENTS
   A. The electromagnetic spectrum of spectroscopy
   B. Frequency measurement

I. THE PROGRAM OF HIGH RESOLUTION SPECTROSCOPY

The program of high resolution spectroscopy (Fig. 1) is to make contact between the physical world, which is a complicated, complex world of many phenomena which are often uncontrollable or not thorougly understood, and the world of physical theory. In this model world, phenomena are described simply. The principles are clear, they can be stated analytically, and they are often idealized. Nonetheless, we can describe a certain body of phenomena approximately by theory. If we want to make contact between the real world and the world of models, one must extend from the clear simple theory of, let us say, solutions of the Schrödinger Equation to more complicated cases where we begin to include real phenomena. At the same time we must make the experiments that we do ever more clear cut, ever cleaner so that they approach more closely the model world. Our hope is to find a meeting ground between the two, in which case we can say we have understood the phenomenon.

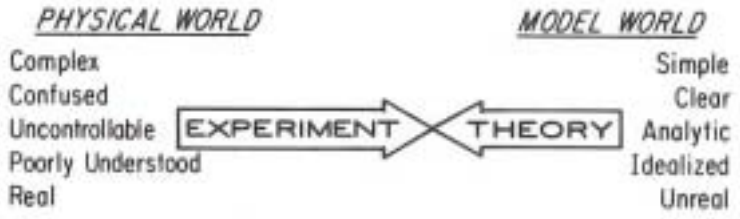

Fig. 1. The program of high-resolution spectroscopy.

What I shall discuss here will be principally the experimental progress in spectroscopy, because, in fact, in recent years experimental progress has been much more dramatic than theoretical progress. Great theoretical progress took place earlier in this century beginning with the quantum mechanical revolution. The next great revolution, and the last one from the point of view of atomic and molecular structure, was the quantum electrodynamic revolution in the late 1940s early 1950s. In very broad terms, one could describe the theory that has been done since as solving the problems that the basic theoretical developments of the 1900s through 1950s gave us. The experimental advances have occurred in two great cycles. The first, which took place from roughly the 1880s through the 1930s, saw the development of vacuum technology, electronics, and modern "conventional" spectroscopic instruments, particularly the diffraction grating spectrometer. The experimenter's technique was "passive" in the sense that he excited the sample in a largely uncontrolled, although perhaps inspired way, and recorded the

results. The second great cycle took place from roughly the 1930s through the 1980s, and is still taking place. It coincided with the development of the laser, the maser, and other coherent radiation sources, neutral and ionic beams, ultrahigh vacuua, low temperature technology, and the digital computer. Its emphasis is on "active" techniques, in which the state of the sample is manipulated in a controlled way in order to achieve a definite, usually preplanned, end.

If we want to make progress in spectroscopy, there are four steps that we must take. First, we must improve the resolution of our instruments. Second, we must improve their absolute accuracy. Third, we must increase their sensitivity. Fourth and last, we will seek to find new applications of the tools which we surely will develop by taking the first three steps. We would like also to test the limits to advancement in steps one, two, and three, to see how far we can go, and to proceed until we are stopped ultimately by laws of nature, such as the uncertainty principle and other basic relations.

II. CONVENTIONAL SPECTROSCOPY

Let us begin by considering conventional laser spectroscopy, which is almost the same as conventional nonlaser spectroscopy. The use of the laser doesn't really contribute too much yet except ease and convenience. There are two basic ways to do spectroscopy. The first way is the so-called absorption method [Fig. 2(a)], in which one shines the light of a laser, or indeed any light source, through a sample containing the atoms or molecules one is interested in studying, and

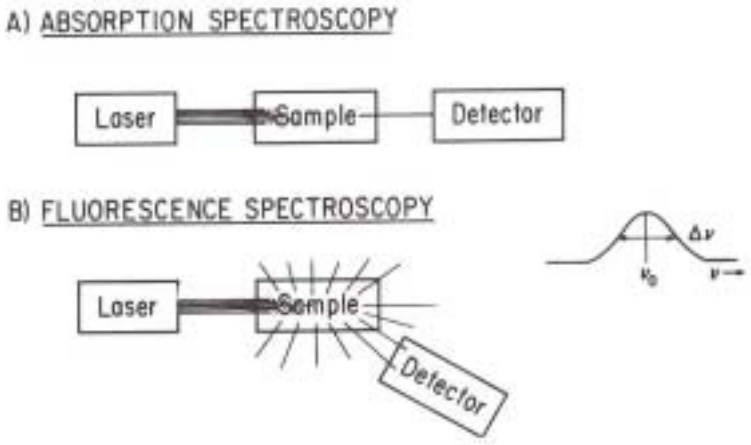

Fig. 2. Conventional spectroscopic methods.

collects the light with a detector of some sort. If one tunes, for example, the frequency of the laser, a region of absorption may appear. Then one can say that at the center of the absorption there is a resonance in the sample, normally corresponding to a transition between two quantum states. The second way is to observe fluorescence [Fig. 2(b)]. One shines the laser beam into the sample, and if the laser is adjusted so that the sample absorbs its light, then the sample may emit

light either at the same wavelength as is absorbed, or at other wavelengths. The detector detects the emission, which is called fluorescence. This detector may be a broadband device such as a photomultiplier; alternately, it may be a wavelength-selective device such as a grating spectrometer. Now one may tune either the laser or the detecting spectrometer in order to investigate the sample's properties.

III. UNCONVENTIONAL SPECTROSCOPY

There is also a growing body of techniques which together are called unconventional spectroscopy, and also often involve lasers. There are many new techniques, several of which we will explore. These techniques are aimed principally at reducing the width of the spectral line and increasing its intensity, or reducing its noise level. In addition, the aim of some is to use the laser's high intensity to induce nonlinear sample behavior unachievable with ordinary light sources. Since our title is "on the limits to precision in spectroscopy," we will not focus on these unless they carry us further toward that goal.

Let us now consider the sources of the width of the spectral line, since the width is the thing that most of the research has been aimed at. I will be treating principally gases rather than liquids or solids, since the highest resolution spectroscopy is done on gases. We may distinguish five different general sources of line broadening in a gas of atoms or molecules (Table I).

Table I. Sources of line broadening in a gas of atoms or molecules.

(1)	Environment
	- Static electric and magnetic fields (Stark and Zeeman Effects)
	- Collisions with other atoms
	- Collisions with walls
(2)	Doppler effect due to atomic motion
(3)	Finite interaction time
(4)	Instrumental broadening
(5)	Coupling to real and virtual background radiation field

The first is the environment of the atoms: Static electric and magnetic fields may be present, and may shift energy levels through the Zeeman effect in the magnetic case, or the Stark effect in the electric case; there may also be collisions with other atoms in the sample, or with the walls, which broaden the spectral lines. There may be a Doppler effect due to atomic motion. There may be broadening due to the finite time that the light interacts with the atomic sample. There may be broadening due to the limits of quality of the instruments one is using. Finally, there may be broadening due to the coupling of the molecule or atom that one is studying to the radiation field. The radiation field has three parts. First is the radiation field of the laser, which will broaden a transition if it is more intense than the minimum which is needed to induce a transition with reasonable probability during the time

available; this is called power broadening. Next is the background radiation field, which has two parts. The real part is what we normally call blackbody radiation - the part of the background radiation field which depends on the temperature. Its total intensity is proportional to the area of the emitting surface times the fourth power of its temperature. There is also the virtual background radiation field, that is, the part of the radiation field which is still present at zero temperature. This is the source of so-called vacuum fluctuations. As we shall see later, it is also the source of spontaneous emission by atoms.

In the next few sections I shall examine the state of the art of reducing these effects to their smallest possible value so as to make the width of the spectral line as small as possible. There has been a great deal of progress in eliminating some of these effects and much less for others. But in principle we know how to eliminate all of them; so some of what I will be discussing is what has already happened and some will be what is likely to happen in the future but has not happened yet.

IV. ELEMENTS OF ATOMIC STRUCTURE: THE HYDROGEN ATOM

Let us now review very briefly the energy level structure of an isolated atom, taking as an example the simplest possible atom, namely the hydrogen atom.[1,2] Its energy level diagram according to the Bohr model is shown in Fig. 3. The ground state, labeled 1, is taken as the zero of energy. The highest bound state lies 13.6 eV above the ground state and is labeled ∞. Above it lies the so-called ionization continuum. In the continuum states the two parts of the atom, the electron and the proton, move near one another but are not bound, so that the electron has the possibility of moving infinitely far away. In the discrete states below the ionization continuum the electron and the proton are bound together and cannot move to infinity. From the viewpoint of classical physics, the light electron would orbit around the heavy proton very much like a planet orbits around the sun. In the ionization continuum the electron would move in a hyperbolic or possibly a parabolic orbit very much like a comet which comes in from infinity, departs, and does not return. In a discrete state, the electron would move in an elliptical orbit like a planet or a recurring comet and would return to pass near the sun once each revolution. Only certain orbits, however, would be allowed. The existence of the discrete energy levels was predicted by the old quantum theory of Niels Bohr early in this century, and has been amply verified since. With the advent of modern quantum theory, starting in 1926, one could describe the energy level structure in great detail, and we believe, in principle, perfect detail.

When an atom drops from one of its excited levels n' to a lower level n, it emits light. In the hydrogen atom the emission lines are grouped into series according to the quantum number of the lower state involved in the transition. The series are named according to their discoverers. The first five series, with $n=1$ through 5, are called Lyman, Balmer, Paschen, Brackett, and Pfund. The members of the series are given Greek letters according to the state change n'-n: α, β, γ, δ, and so

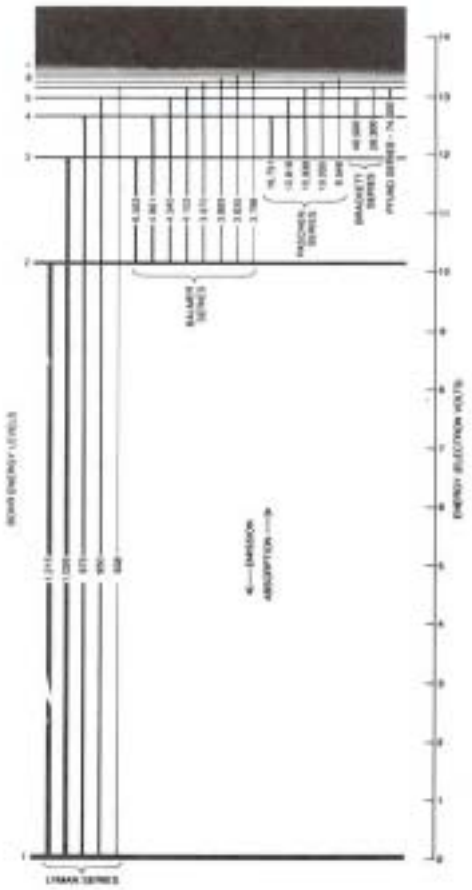

Fig. 3. Energy levels and important transitions in atomic hydrogen (adapted from Ref. 2.).

on, corresponding to 1, 2, 3, 4, and so on. Thus the first line, from 2 to 1, is called the Lyman-alpha line, and the next one, from 3 to 1, is called Lyman beta. The Lyman series is in the ultraviolet and normally is not seen, because the light will not pass through the glass walls of a discharge tube. But one can see the Balmer lines, which are in the visible. The first one, from 3 to 2, is Balmer alpha, also called H alpha, and is red. The next, Balmer beta or H beta, from 4 to 2, is blue. The third, H gamma, from 5 to 2, is deep violet; the rest are ultraviolet. The higher series all lie in the infrared. Most of the research on hydrogen has been done on the Balmer lines because you can see them.

If one looks at the details of the hydrogen spectrum more carefully, one finds that each of the energy levels is shifted slightly from the Bohr position, and is split into several sublevels. As each higher level of detail is revealed, a more precise theory is needed to account for it. Figure 4 shows this progression. On the left we have the positions of the energy levels according to the original theory of Bohr in 1913.[4] In 1928 P.A.M. Dirac made an improved quantum theory[5] including the effects of special relativity. His hydrogen energy levels are shown second from the left. The lowest level has shifted downward and has also gained a new quantum number, the 1/2, which represents the spin of the electron, and appears as a natural consequence of his theory. All the levels gained this extra angular momentum. In the late 1930s and early to late 1940s, the theory of quantum electrodynamics (QED) was

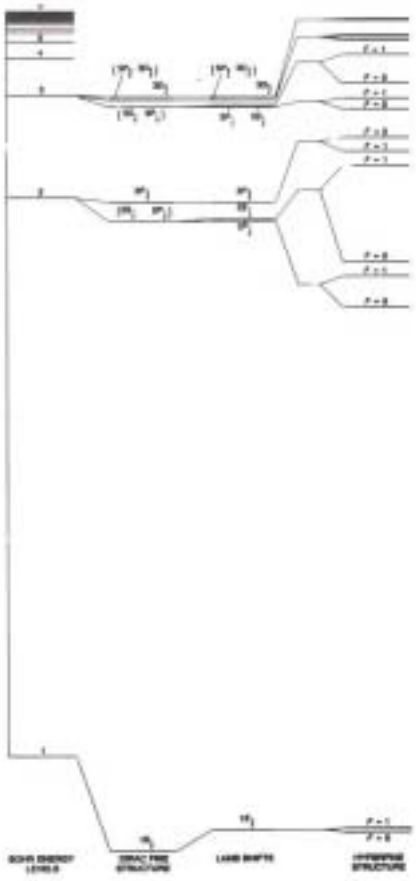

Fig. 4. Evolution of hydrogen energy levels with refinement of theory (from Ref. 3).

developed by Feynmann,[6] Schwinger,[7] Tomonaga,[8] and others. They received the 1965 Nobel prize for their work. One result of their theory (third from left) is that the S levels, which have zero orbital angular momentum, are shifted upward slightly because of the interaction of the atom with the virtual fluctuations in the vacuum radiation field that are present even at 0 K when the blackbody field intensity has dropped to nothing.

The famous n=2 state has been studied the most. In it, and in all the higher states, there is a possibility that the electron's orbit will, classically speaking, have a net "circularity," so that the atom will acquire an orbital magnetic moment from the revolving of the charged electron. The electron's intrinsic spin magnetic moment interacts with the orbital moment; the interaction depends on the relative orientation of the two moments, and hence of the two angular momenta. The so-called 2P states have angular momentum L=1, in units of $\hbar$, and the electron's spin angular momentum is S=1/2, giving possible total angular mommenta values J of L+S=3/2 and L-S=1/2. Here $\hbar$ is Planck's constant h divided by 2π. Thus the 2P state has two sublevels, $2P_{1/2}$ and $2P_{3/2}$, whose energies differ by the change in the magnetic moments interaction. There is also a $2S_{1/2}$ state, whose electron orbit according to classical physics would go back and forth through the nucleus, or according to quantum theory, has a spherically symmetric wave function. In the Dirac

theory the $2S_{1/2}$ state and the $2P_{1/2}$ have exactly the same energy, but in quantum electrodynamics they are slightly split by the S-state shift (and by a very small P-state shift). This shift, which is about 1000 MHz in n=2, is called the Lamb shift, after W. E. Lamb, who discovered it in 1947 with a very beautiful experiment done by him and his co-worker R. C. Retherford.

At about the same time, P. Kusch discovered that the magnetic moment g of the electron was not exactly two Bohr magnetons, as the Dirac theory predicted. This "anomalous magnetic moment" g-2 was also explained successfully by the quantum electrodynamic theory. These discoveries, which stimulated the development of quantum electrodynamics, led to the awarding of the Nobel prize to Lamb and Kusch in 1955.

Finally, if the nucleus has a spin (1/2 for a proton), the energy levels split again; the $1S_{1/2}$ lowest level, which we have been following, splits into two sublevels having F=1 and F=0, where F is the total angular momentum of the atom in units of $\hbar$. These splittings are called hyperfine structure and are shown at the right, with the vertical scale expanded.

Other atoms have different structural details, but the hydrogen atom is a simple and sufficiently representative case that we can refer to it again from time to time in order to give concrete applications of the spectroscopic techniques we will examine.

V. ESTIMATES OF LINE BROADENING EFFECTS IN CONVENTIONAL SPECTROSCOPY

Let us next consider some details of the line broadening effects listed in Table I. To be definite, let us imagine that we wish to study the red Hα (n=3 to n=2) transition of atomic hydrogen using either of the conventional spectroscopic methods shown in Fig. 2. Its wavelength is about 6×10^{-5} cm (actually 6563 Å), and the speed of light is about 3×10^{10} cm/sec. The optical frequency is then

$$\nu = c/\lambda = 3\times10^{10} \text{ cm/sec} \div 6\times10^{-5} = 5\times10^{14} \text{ Hz}. \qquad (1)$$

This is a very, very high frequency compared to that of, let us say, a radio wave or a television signal. Still, it is not impossibly high, and we will see later on how with very new developments in technology people are able to measure frequencies like this directly.

A. Effects of atomic motion

Let us first investigate the effects of atomic thermal motion. To begin we must calculate what a typical speed v is for a hydrogen atom. The average kinetic energy $Mv^2/2$ of each dimension of motion for an atom in a gas sample which has absolute temperature T is kT/2, where k is Boltzmann's constant. Dividing by the rest energy Mc^2 and applying a small amount of algebra results in

$$v/c = (kT/Mc^2)^{1/2} . \qquad (2)$$

This v is the root-mean-square value for motion in one direction. At ordinary temperature (T=300 K), kT=0.025 eV. By comparison, the rest energy of the hydrogen atom is about 10^9 eV. Putting these numbers into Eq. (2), we find that v/c is 5×10^{-6}, and the velocity is 1.5×10^5 cm/sec. This is about the speed of a very fast rifle bullet, and it is also about equal to the speed of sound in a gas of hydrogen atoms. Of course there is a very good reason why that is so, namely that sound propagates in a gas with a speed about equal to the speed of the atoms in the gas. Since hydrogen is the lightest atom, this speed is the fastest you would find in any gas at room temperature. M is about 30 times greater for air, for example, so the molecular speed in air would be about 5 or 6 times lower. A speed in the range of 10^4 to 10^5 cm/sec is typical for most atoms and small molecules. The actual distribution of speeds is the Maxwell-Boltzmann distribution, which is shown in Fig. 5.

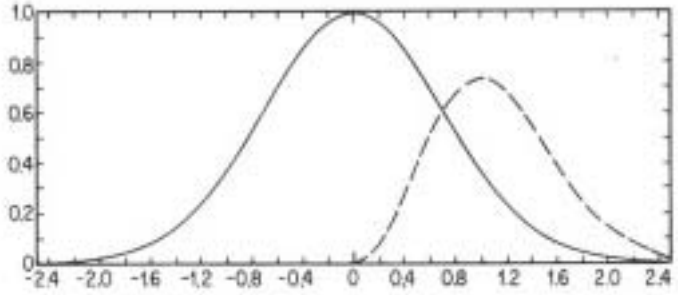

Fig. 5. One-dimensional (solid curve) and three-dimensional (dotted curve) Maxwell-Boltzmann distributions of atomic velocity in an ideal gas. Ordinate: relative probability. Abcissa: speed in units of $(kT/M)^{1/2}$.

1. Collisions

The "perpetual motion" of the atoms has several effects. First, if the atoms are moving rapidly and randomly, they will hit each other often. Let us calculate a collision rate using a density of atoms corresponding to a pressure of 1 Torr, which is a typical pressure in a gas discharge atomic light source. One Torr is approximately 1/760 of an atmosphere, so the number of molecules at 1 Torr in the room in which you are reading this would be 1/760 of the number there are at the present time. The number R of collisions per second that any atom receives is equal to the density ρ of other atoms times the cross section σ for collisions (the effective area for the collision which the atom presents to the others bombarding it) times the mean relative speed v_{rel}. This speed is roughly the speed v we have just calculated, times $\sqrt{6}$. The $\sqrt{6}$ converts from one dimension of motion for one atom to three dimensions of motion each for two atoms. Thus

$$R = \rho\sigma v\sqrt{6} \ . \qquad (3)$$

We may assume that the radius for a broadening collision between an atom in state n and an atom in state 1 is about the same as the sum of the

geometric radii of the two atoms: $r=n^2a_o+a_o$, where $a_o=5\times10^{-9}$ cm is the Bohr radius, or the classical radius of the ground-state orbit. Then we have

$$\sigma = \pi r^2 = \pi(n^2 + 1)^2 a_o^2 . \tag{4}$$

To find the density ρ we can use the fact that one mole of any gas occupies 22,400 cm^3 at standard conditions, (760 Torr pressure, 273 K) and contains 6.02×10^{23} atoms. Thus at 1 Torr and 300 K, the density is

$$\rho = \frac{(6.02\times10^{23}\ \text{atom mole}^{-1})}{(2.24\times10^{4}\ \text{cm}^3\ \text{mole}^{-1}\ \text{atm}\text{-}273\ \text{K})(760\ \text{Torr atm}^{-1})}\left(\frac{273\ \text{K}}{300\ \text{K}}\right)$$
$$=3.2\times10^{16}\ \text{atom cm}^{-3}. \tag{5}$$

If we do the calculation for the upper state of the Hα line, n=3 in Eq. (5). Putting in all the other numbers gives $R=9\times10^7$ collisions per second. When the atom suffers a collision during the process of absorbing or radiating emitting light, the phase of the electric field oscillation that the atom emits is interrupted. As a result, the Fourier transform of the wave train shows a broadening which is approximately

$$\Delta\nu_c = R/2\pi = 1.5\times10^7\ \text{Hz} . \tag{6}$$

A more detailed model of the collision would give a somewhat different numerical value, but this is a reasonable order of magnitude.

2. Doppler broadening

Next let us look at Doppler broadening. It is known that the observed frequency of a wave shifts if the observer is moving toward or away from the source of the wave. The nonrelativistic expression for the shift is

$$\nu(v) - \nu(0) = (v/c)\ \nu(0) . \tag{7}$$

where v is the velocity along the line of sight. Because the atoms in our gas have their velocities spread over a range about equal to 2v (Fig. 5), there will be many different values of the Doppler shift of the light emitted by the atoms in the sample. Thus we will have a Doppler broadening $\Delta\nu_o$ of the spectral line which is given approximately by

$$\Delta\nu_o = 2(v/c)\ \nu . \tag{8}$$

For $v/c = 5\times10^{-6}$ and a frequency of 5×10^{14} Hz, $\Delta\nu_o$ will be 2.5×10^9 Hz. You can see already that this effect is much larger than the collisional broadening, at least for the conditions I've shown. It will in fact turn out to be the largest broadening effect in most spectroscopic experiments which use the methods of Fig. 2.

3. Transit broadening

The next effect is called transit broadening, which is closely related to the uncertainty principle, or to the Fourier transform of a

sinusoid. If a sinusoidal oscillation goes on for an extremely long time, its frequency spectrum, which is its Fourier transform, is extremely sharp. However, if a piece of the oscillation is cut out and isolated so that the amplitude is zero before and afterward, then the Fourier transform of the piece has a definite width $\Delta\nu_T$ (T for transform or transit) which is equal to the reciprocal, divided by 2π, of the time that the wave is turned on.

If a moving atom is illuminated by a laser beam, the atom will feel a pulse of light whose duration is equal to the time that it spends in the beam. That time is longer for some atoms and shorter for others, but is typically about equal to the root-mean-square one-dimensional speed v of the atom divided by the radius of the beam. Thus

$$\Delta\nu_T = v/2\pi R_{beam} . \tag{9}$$

For a speed v of 1.5×10^5 cm/sec and a laser beam of 2 mm radius, $\Delta\nu_T = 10^5$ Hz.

The next effect that adds to the linebreadth is the decay of the atomic states by spontaneous emission. The spontaneous emission, or "natural" broadening of an atomic energy level is

$$\Delta\nu_n = 1/2\pi\tau , \tag{10}$$

where τ is the lifetime of the state. If both the upper and lower states of a transition decay, we must add their linewidths to get the total broadening. This broadening source is again a result of the uncertainty principle, and can also be obtained from the Fourier transform of an exponentially decaying wavetrain whose intensity drops by the factor e=2.718... in time τ. Some typical values for the spontaneous emission broadening in hydrogen are: For the Hα 3P-2S transition, 3×10^7 Hz. For the Lα 2P-1S transition, 1×10^8 Hz. For the 2S-1S transition, 1 Hz. The reason the last number is so small is that the 2S state is metastable and cannot emit light in the electric dipole approximation. It radiates primarily by a "forbidden" 2-photon process, which is very slow. There are other states as well whose decay is very slow; these are the high-lying Rydberg states whose principal quantum number n is much greater than 1. The essential point to remember is that different states of an atom can have lifetimes differing by many orders of magnitude.

B. Stray quasistatic fields

Next, let us look into the effects of stray electric and magnetic fields. If our sample is, for instance, a discharge tube with a current flowing through it, like the neon signs that we see in downtown Taipei, there will be both an electric field **E** and a magnetic field **B** in the discharge. The electric field is required to keep the current flowing in the presence of collisional kinetic energy losses, and is typically on the order of 10-100 V/cm. It will cause a shift of the energy levels, the so-called second-order Stark effect from quantum theory, and if the

field is nonuniform it will also cause broadening. The shift of any state a is

$$\nu_a(\mathbf{E})-\nu_a(\mathbf{0}) = \sum_b \frac{|\langle a|e\mathbf{E}\cdot\mathbf{r}/h|b\rangle|^2}{\nu_a - \nu_b} , \qquad (11)$$

where $\mathbf{r}$ is the electron's coordinate in the atom and ν_a, ν_b are the atoms' energy levels in Hz. As an example, I will work out the order of magnitude of the shift for the 2S state of hydrogen. Earlier we saw that in hydrogen the $^2P_{1/2}$ state and the $^2S_{1/2}$ state have no energy difference in the Dirac theory, but actually they are split by about 1000 Mhz. This is a very, very small energy difference compared to most atomic energy differences. Therefore, what I will calculate here will be an exceptionally large shift.

In electrostatic units, the charge on the electron is 4.8×10^{-10} esu; the electric field is 1/30 to 1/3 sV/cm; for the matrix element of r we can use the radius of the n=2 state, which is $2^2a_o=2\times10^{-8}$ cm, and Planck's constant h is 6.6×10^{-27} erg-sec. With h in the formula, the numerator in Eq. (11) is in Hz^2 and the denominator is in Hz, so we have a consistent set of units. When we put the numbers in, we find that the second-order Stark shift is approximately 2×10^6 to 2×10^8 Hz - about the same size as the other smaller effects - and the broadening $\Delta\nu_S$ will be whatever fraction of this the spread in E^2 gives, perhaps 1/2 to 1/4 of the shift.

The discharge current of, say, 10 to 100 mA spread over a column of about 1 cm diameter will produce a magnetic field, but the 0.5-gauss magnetic field of the earth will be somewhat larger. The field will split the Zeeman components of each energy level, and cause a symmetrical broadening $\Delta\nu_Z$ of the spectral line which amounts to roughly

$$\Delta\nu_Z = 2(\mu_B/h)B = (e/2\pi mc)B , \qquad (12)$$

where $m(=9.1\times10^{-28}$ g) is the electron's mass and μ_B is the Bohr magneton. Putting in the numbers yields $\Delta\nu_Z \approx 10^6$ Hz.

C. Rapidly varying stray fields

Finally we must consider the effects of the rapidly time-varying fields the atom is subjected to. These fields are the field of the laser beam illuminating the sample, the field of the thermal or "blackbody" radiation in the apparatus, and the long-range time-varying fields of the ions and electrons in the sample if the sample is a gas discharge. It is quite accurate to consider only the electric fields of these sources, and to neglect their magnetic fields, because the latter is at most of the same order of strength as the former, and the magnetic interaction $\boldsymbol{\mu}\cdot\mathbf{B}$ is therefore weaker than the electric interaction $e\mathbf{E}\cdot\mathbf{r}$ at least by a factor on the order of $\mu_B/ea_o=\alpha=e^2/\hbar c=1/137$. These fields can cause Stark shifts which are qualitatively similar to, but usually smaller than, the static-field Stark shift we have just estimated. Their nonuniformity will then cause broadening. In addition, they can cause

broadening by inducing transitions between states, and hence shortening the states' effective lifetimes. The laser field broadening is called power broadening, and can be adjusted by the experimenter; in order to bring a resonance signal to full strength, it may be necessary to set the power broadening about comparable to the largest of the other broadening mechanisms, but rarely more.

1. Of thermal radiation

The blackbody electric field present in this room at 300 K temperature amounts to about 10 V/cm root-mean-square, integrated over the entire spectral distribution. Its effects can easily be sensed if you put your hand, or a mirror, near to your cheek but not touching it. Since your hand or the reflection of your face is warmer than the surrounding objects, your cheek will feel warm. Since on the thermal radiation energy is spread over a wide range of frequencies, calculating the effects accurately requires some analysis.[9,10] The results of these studies for the 2S state of hydrogen[10] appear in Table II.

TABLE II. Theoretical blackbody radiation effects on the 2S state of the hydrogen atom.

	300 K	3000 K
Shift =	-1.08 Hz	-1.5×10^{4} Hz
Broadening ($\Delta\nu_{BB}$) =	1.4×10^{-5} Hz.	7×10^{4} Hz

It is interesting to note that there should be a connection between the blackbody radiation effects and the spontaneous emission effects, since they originate from different parts of the same radiation field. This connection will be brought out more clearly further on.

2. Holtzmark broadening

The effect of long-range ion and electron fields is called Holtzmark broadening. It depends greatly on the details of the discharge operation, but in general will be of the same order of size as, or smaller than, the static field Stark broadening, and henceforth will be subsumed under that heading.

D. Summary

The results of the above discussion are summarized in Table III. Although these numbers were calculated for the hydrogen atom Hα line, for many other atoms and spectral lines they should not be more than a factor of ten or so larger or smaller.

Table III. Estimated broadening and shift of the H_α line in conventional spectroscopy.

Operating conditions:		
Temperature	300 K	
Pressure	1 Torr	
Discharge current	10-100 mA	
Discharge diameter	1 cm	
Electric field	10-100 V/cm	
Magnetic field	0.5 gauss	
Perturbing effects:	Broadening (Hz)	Shift (Hz)
Neutral collisions	$\Delta\nu_c = 1.5\times10^7$	
Thermal motion	$\Delta\nu_D = 5\times10^9$	
Transit through laser beam	$\Delta\nu_T = 10^5$	
Spontaneous emission	$\Delta\nu_n = 10^7$	
Electric fields	$\Delta\nu_S = 5\times10^5$-$10^8$	2×10^6-2×10^8
Magnetic fields	$\Delta\nu_Z = 10^6$	
Blackbody radiation	$\Delta\nu_{BB} = 4\times10^{-4}$	-12

VI. REDUCTION OF DOPPLER BROADENING

Evidently the largest effect in Table III is the Doppler broadening, which is on the order of 10^9 Hz and is very, very large compared to many of the others. The first thing that one must do if one wishes to increase the resolution of spectroscopy is to find a way to eliminate the Doppler broadening - some way to see the spectrum of the atom without seeing the broadening which comes from the motion of the atom. People have devised many different techniques to eliminate or reduce the Doppler broadening. Some of these are quite ingenious, and some of them produce remarkable results in resolving the spectrum. We will examine the most important methods. Then, when we have eliminated the Doppler broadening, we will turn to the other smaller effects to see how we can eliminate them as well.

Let us first look more precisely at what the Doppler broadening effect depends on. Consider a photon propagating in some direction with a propagation vector **k** (Fig. 6). This **k** is the angular frequency $\omega=\nu/2\pi$ of the photon, divided by the speed of light c, times the unit vector $\hat{z}$,

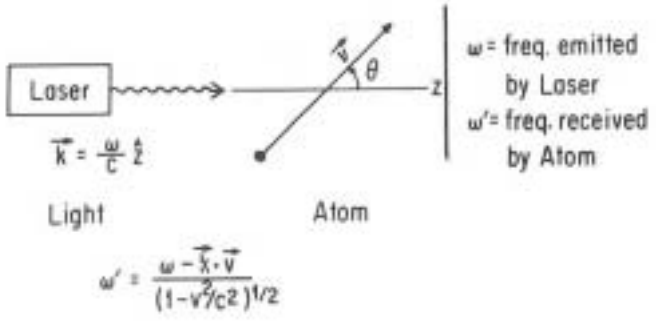

Fig. 6. Doppler effect in light-atom interaction.

which points in the direction that the photon is moving. Then the magnitude of k is the number of radians of the electromagnetic oscillation per centimeter of travel. The photon interacts with an atom moving at a velocity **v** in some other direction, and the angle between **k** and **v** is θ. The exact expression for the Doppler effect is

$$\omega' = \frac{\omega - \mathbf{k}\cdot\mathbf{v}}{(1-v^2/c^2)^{1/2}} = \omega \frac{(1-v\cos\theta/c)}{(1-v^2/c^2)^{1/2}}, \qquad (13)$$

where ω′ is the frequency that the atom experiences. In most elementary textbooks the formula is written without the $(1-v^2/c^2)^{1/2}$ factor in the denominator because most elementary textbooks neglect the theory of relativity. Including this factor expresses the change in time scale between the inertial frame in which the atom is at rest and the inertial frame in which the laser is at rest. What we would like to do is to find some experimental way to reduce this effect to the smallest possible value.

Our starting point must be the **k**•**v** term, since the strongest velocity dependence appears there. We may try to eliminate it, or just to reduce its spread of values. The possibilities then are (a) to reduce the value or the spread in v; (b) to reduce the value or the spread in cosθ; and (c) to reduce the value or the spread in k (normally its spread is already quite small). The many different methods of "Doppler-free spectroscopy" all reduce one or more of those quantities.

A. Temperature reduction

To reduce v or its spread, the first and most obvious method is to lower the temperature, because the velocity comes from the thermal motion of the atoms. This is an old method; for example, many years ago the hydrogen Hα line was studied in a discharge cooled with liquid nitrogen in order to measure the Rydberg constant. Ultimately this method has a limit, because if you cool things too much they freeze, and then all the atoms disappear from the vessel and end up on the walls, and you have no more atoms to study. How much one can cool depends on the vapor pressure of the material you are working with. Since hydrogen has a very high vapor pressure of about 1 atm at 20 K, one could perhaps cool to even 10 K and still have a sample dense enough to do spectroscopy with. But many other substances, e.g., iron or magnesium, are solid even at room temperature, and so the sample must be quite hot in order to be useful. Later we will look at the technique of atom trapping, which allows cooling without freezing in some cases.

B. Mass increase

Another possibility to reduce v would be to study only very heavy atoms, because v varies as $M^{-1/2}$ at constant temperature. Unfortunately, the simplest and hence the most fundamental atoms, hydrogen or helium, are very light, and even though an improvement in resolution of the hydrogen spectrum is achieved by using the heavier deuterium isotope, the resolution increase gained thereby is relatively modest.

These two methods are what one might call the "traditional" methods. Recently, a large number of new "modern" methods of velocity broadening reduction have come into use, which have proved to be much more effective. Let us now look at them.

C. Fast-beam kinematic compression

The next method, which was developed by my co-workers and myself at the University of Arizona,[11-17] is to accelerate the atom. It may not seem that if one makes the atom faster, the velocity broadening of its spectrum should be lower. In fact, this is possible using an apparatus such as that shown in Fig. 7. A sample of ions is accelerated to form a

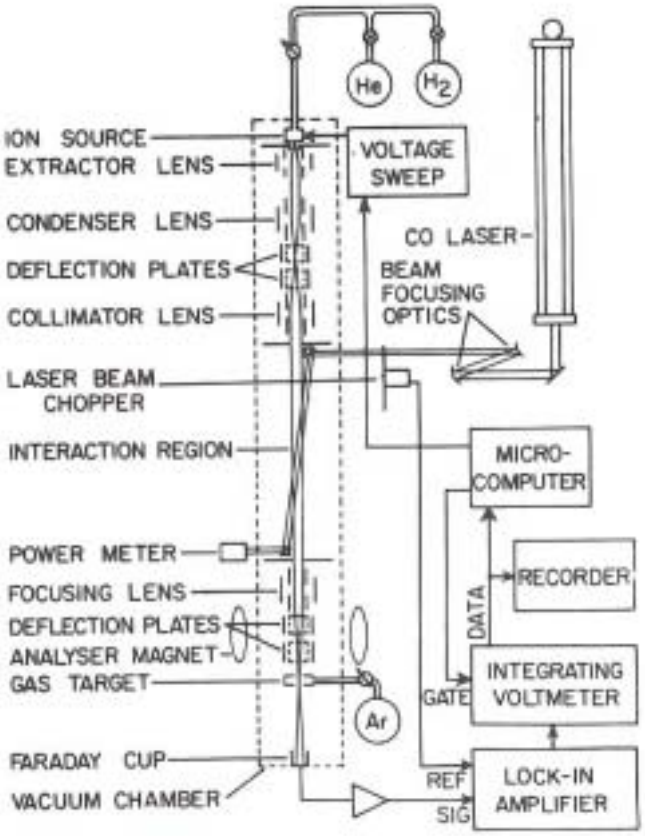

Fig. 7. Fast beam laser Doppler-shift spectrometer (from Ref. 14). Gases are as chosen for study of the HeH^+ molecular ion.

collimated beam and is illuminated by a nearly co-parallel laser beam. One or another effect of the light on the ions is used as a detection mechanism; here it is the change in charge-exchange cross section that accompanies a change of internal state. Let us look at how the spread in velocity behaves. Conservation of energy during acceleration requires

$$\frac{1}{2}mv^2 = \frac{1}{2}mv_o^2 + qV \ , \tag{14}$$

where v_o and v are the initial and final speeds and qV is the kinetic energy that the accelerating voltage supplies. Taking the derivative at constant V, we find

$$v\delta v = v_o \delta v_o \ . \tag{15}$$

So the spread of velocities δv in the moving beam, which has perhaps several keV of kinetic energy, is equal to the initial spread of velocities δv_o times the ratio v_o/v. But the initial velocity v_o is quite slow since the initial kinetic energy of the ions in the source may be of the order of 1 eV, whereas the final velocity is quite fast. Therefore v_o/v is small compared to 1, which means that the velocity spread has been reduced by the acceleration process. This technique, which is called "kinematic compression," produces very sharp resonance lines. Figure 8 is an example of such a resonance line for the hydrogen molecular ion HD^+. The beam voltage is proportional to the frequency of the laser beam ω' that is experienced by the moving ion. Some of the hyperfine structure in the transition has been resolved; without kinematic compression the line would have been 20 to 100 times broader.

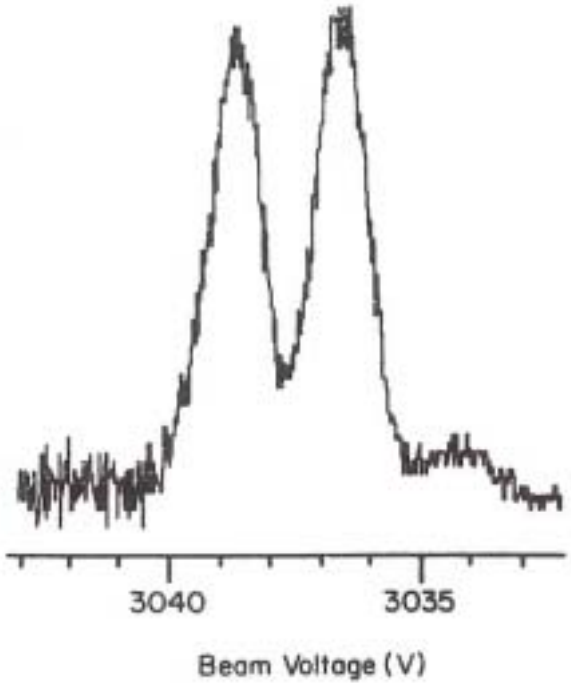

Fig. 8. Fast beam Doppler-shift laser resonance trace of the (v=1, N=1)-(v=0, N=2) transition in the HD^+ ion (from Ref. 11).

D. Saturation spectroscopy

The technique of saturation spectroscopy has been used very widely in recent years. To understand the essential features, let us imagine placing the atomic sample in a standing wave optical field, so that it can be thought of as interacting with not one but two beams traveling in opposite directions with propagation vectors $+\mathbf{k}$ and $-\mathbf{k}$. A sample atom traveling at a velocity $\mathbf{v}$ will see two frequencies, which are $\omega+\mathbf{k}\cdot\mathbf{v}$ and $\omega-\mathbf{k}\cdot\mathbf{v}$, if special relativity is neglected. As long as $\mathbf{v}$ is not zero, these frequencies are different, and the atom will be able to resonate with, at most, one of the beams. Therefore two groups of atoms, having velocities along the laser beam direction of

$$v_z = \pm c(\omega_o-\omega)/v \tag{16}$$

interact with the light, where ω_o is the atom's transition frequency in its rest frame. Only in the special case that the laser is tuned to the atomic frequency ($\omega=\omega_o$) can the same atoms interact with both beams. Those that do have $v_z=0$, and so this gives us a way to eliminate the Doppler broadening if we can find out how to exploit it. To do that, we make the light strong enough to partially bleach, or render transparent, the atomic sample. The resulting population distribution is shown in Fig. 9(b). The normal Boltzmann distribution of ground state atoms has two "holes" burned in it at the two values of v_z [Eq. (16)], where some of the

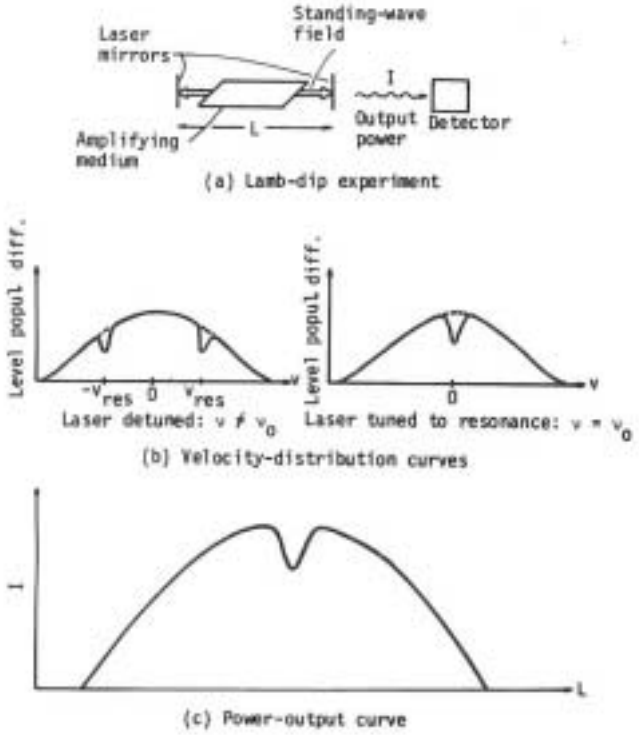

Fig. 9. Lamb dip or saturation dip in laser tuning curve.

atoms are excited. This situation is shown at the left. If one adjusts the frequency of the laser to interact with atoms that are stationary, the population distribution will look as shown at the right. The maximum absorption is twice as great when there are two different populations which can absorb light when there is only one. The absorption "dip" at $\omega=\omega_o$ has a width which is equal to the resultant of all the broadening mechanisms we discussed earlier except Doppler broadening. Of course, this technique gives no signal when the light is very weak, because then there is in effect an infinite supply of atoms regardless of how the laser is tuned. If the sample is a laser medium [Fig. 9(a)], the curves apply to the inversion, or the population difference between upper and lower states. The laser output power then shows a small dip in the center of its tuning curve [Fig. 9(c)]. This output power dip was first predicted theoretically by Lamb[18] and observed by McFarlane, Bennett, and Lamb[19] in the early 1960s, and is known as the "Lamb-Bennett dip."

A spectrometer based on this principle was developed by T. W. Hänsch et al. of Stanford University (Fig. 10).[20] Here we have one beam stronger than the other. The beam splitter S diverts a small percentage of the light, called the probe beam, which goes through the sample cell and

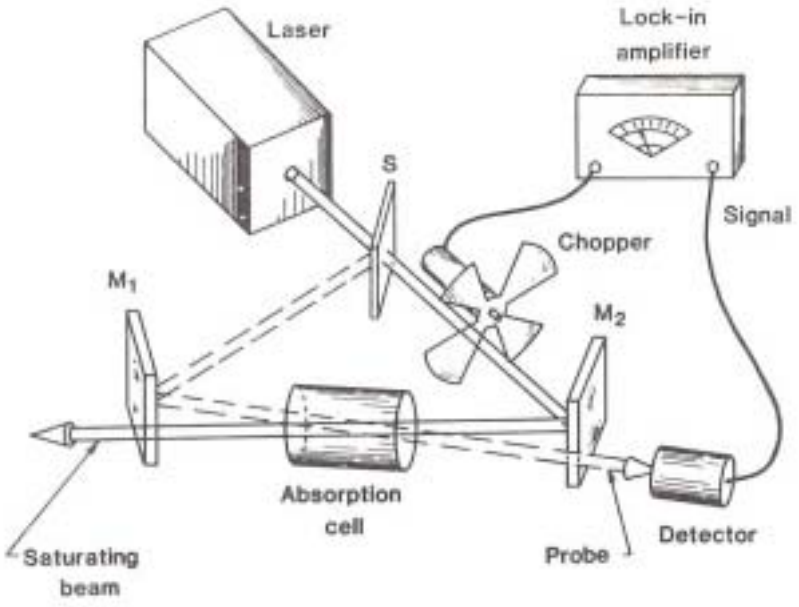

Fig. 10. Saturation spectrometer (from Ref. 3).

into a photodetector. The main part of the light, called the saturating beam, goes through in the opposite direction. If different atoms interact with each beam, then when a light chopper turns on the saturating beam, there is no effect on the probe beam. However, if the same atoms interact with the two beams, which means that they are moving in a plane normal to the mean axis of the beams, then when the saturating beam is turned on, it reduces the number of atoms that can absorb light from the probe beam, and the probe beam, as viewed by the photodetector, gets stronger. Just as before, this occurs when the laser

frequency equals the rest-frame atomic frequency, and the width of the resonance in the probe light is given by the other broadening effects, excluding the Doppler broadening.

Figure 11 shows an example of a result from a spectroscopic experiment that was done on the hydrogen Hα lines by this group.[3] At the top of the figure, the sublevels of the n=2 and n=3 states are shown in detail. There are many different transitions because of the fine structure sublevels. In an ordinary spectrographic experiment on a discharge containing hydrogen, the line profile will look something like that shown in the middle of the figure. Each line is a composite of several transitions. The splitting between the two peaks is approximately equal to the fine structure splitting in the n=2 state, but clearly the situation is quite a bit more complex than that. None of the individual transitions are resolved, and so one has a hard time studying the fine splittings of the states. This sort of spectrum was seen for many years in the spectroscopy of the earlier part of this century, and gave very little hint that buried within it was an essential clue to quantum electrodynamics.

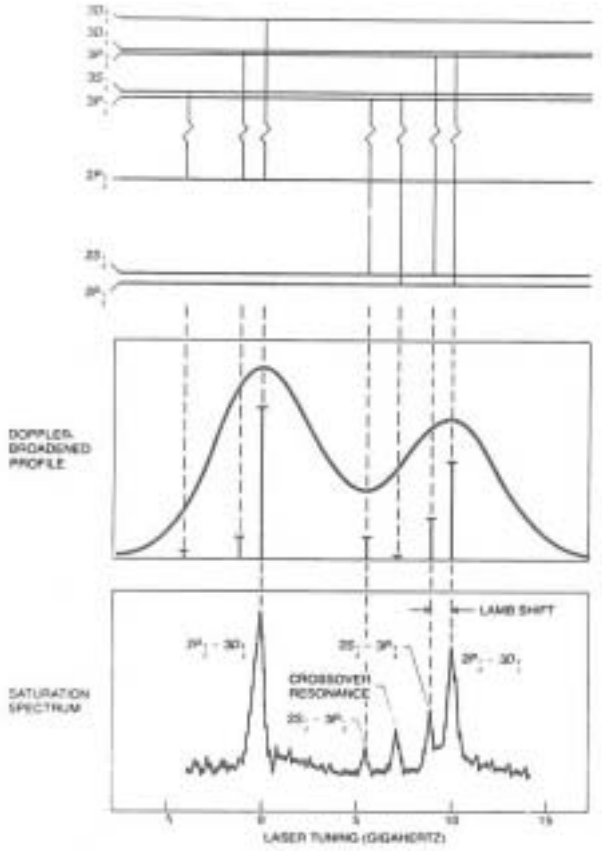

Fig. 11. Saturation spectrum of atomic hydrogen (from Ref. 3).

At the bottom of Fig. 11 is the saturation spectrum. By measuring the distance between the transitions, one can determine the fine structure splittings with reasonable accuracy. In particular, the splitting between the rightmost two lines is very nearly equal to the famous Lamb shift, which, it should be pointed out, was measured by Lamb and co-workers[21] much more accurately over two decades earlier, using a direct microwave resonance method. The real value of this particular saturation experiment was its demonstration of a new way of atomic hydrogen spectroscopy. The "crossover resonance" is an artifact of the method which I shall not discuss.

The results of a very similar experiment that was done by Prof. A. L. Shawlow and colleagues,[22] also at Stanford, is shown in Fig. 12. In this case the object under study is the iodine molecule. Because the $^{127}I_2$ molecules' mass is 254 times that of the H atom, its thermal velocity is about 16 times less at the same temperature. Thus the Doppler profile of its visible spectral lines will be typically 300 MHz wide instead of the 5 GHz hydrogen value we see in the middle curve of Fig. 11. However, the saturation spectrum linewidths of Fig. 12 are only about 20 MHz wide. The narrowing factor of 15 is enough to reveal many

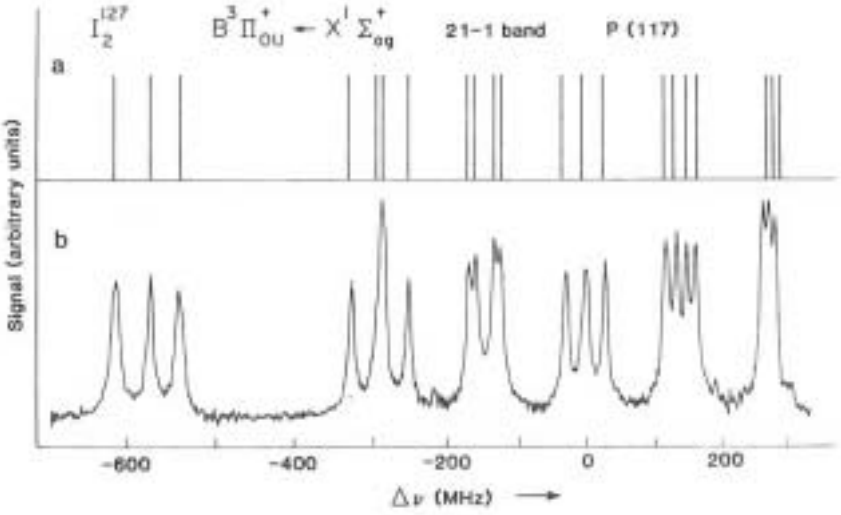

Fig. 12. Saturation spectrum of molecular iodine (from Ref. 3).

rotational sublevels in the iodine molecules. Thus, as with other line-narrowing methods, the saturation spectrum shows fine details which the ordinary Doppler-broadened spectrum cannot show. This technique has been used now in many different spectroscopic studies.

Figure 13 shows a small variation of the technique, which is called polarization spectroscopy.[23] It is basically the same method as before, except that instead of turning on and off the saturating beam with a shutter, one puts a birefringent crystal in it, which converts it to circular polarization. The probe beam is linearly polarized by the first polarizing filter, and so may be decomposed into a sum of two circularly

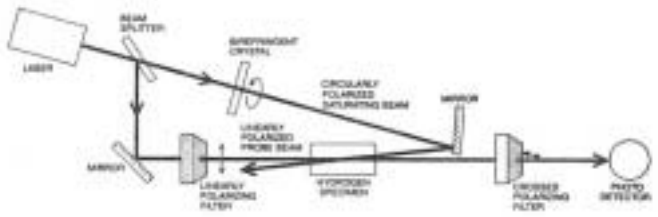

Fig. 13. Polarization-saturation spectrometer (from Ref. 3).

polarized waves of opposite polarization. When they are recomposed by the second crossed polarizing filter, their phases add so as to create a wave polarized parallel to the first filter's axis. The second filter blocks this completely, so no light reaches the photodetector. When the laser is tuned to resonate with zero-v_z atoms, the saturating beam makes the absorption of the two circularly polarized probe beam components unequal. Then when the probe beam is reconstructed at the crossed filter, a certain amount of it manages to pass through and reach the photodetector, giving a signal. Figure 14 shows an example of the results. Again, let us neglect the crossover resonances. At the top of the figure is a saturation spectrum taken with a pulsed laser, similar to that in Fig. 11. Next is one taken with a continuous laser. At the bottom is the polarization spectrum. The signal-to-noise ratio is higher in the continuous case than in the pulsed case because the continuous laser's amplitude was more stable than was the pulsed laser's pulse amplitude. The polarization spectrum has slightly higher signal-to-noise still, because the laser and hence its amplitude noise are completely

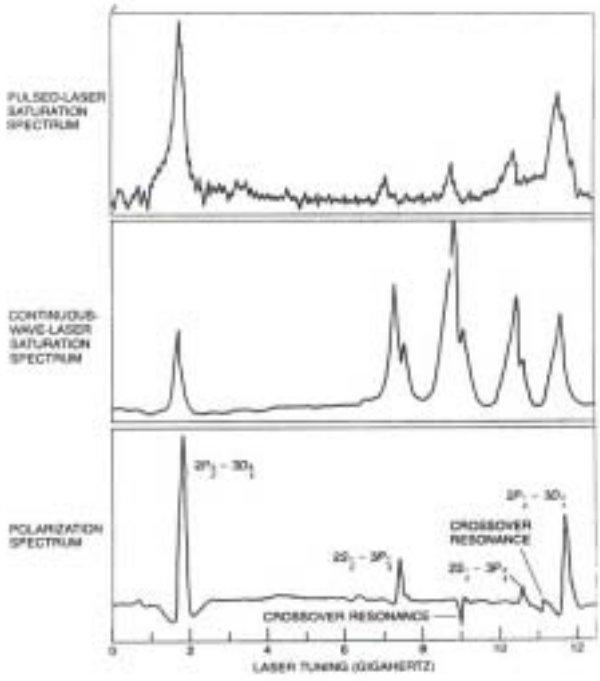

Fig. 14. Polarization-saturation spectrum of atomic hydrogen (from Ref. 3).

blocked between resonances. In addition, the polarization lines are sharper than the saturation lines. In fact, a close look shows that the polarization resonance consists of a weak, broad negative signal combined with a strong, narrow positive one. Qualitatively, the reason for this is that in the polarization method the strong saturating beam power-broadens only one of the two circular components of the atomic transition, whereas in the saturation method it power-broadens both components.

There are several useful variations of the saturation technique. It has one major drawback, which is that to get the narrow resonance it throws away most of the atoms: Only one small velocity group is in resonance, and the other atoms are not part of the signal. So if only a very small number of atoms is available, then the signal may be quite weak. The fast-beam method discussed above does not suffer from this defect, nor do the next two methods to be discussed.

E. Right-angle interaction

This is a very straightforward method. One merely sends the atoms in one direction in a beam and the light in another direction in another beam and fixes the angle θ between them at 90°. Since the Doppler shift is $\mathbf{k}\cdot\mathbf{v} = kv\cos\theta$, at 90° the shift is zero. In reality it won't be precisely zero because there is always a spread in angles in each beam; however, the spreads can be quite small in a well-designed experiment. This idea is actually quite old, but was revived recently and refined significantly by Lichten and co-workers[24] at Yale University. Figure 15 shows their arrangement. The resonance signal is seen by turning on and off the laser with a light chopper and monitoring the change in flux of metastable atoms or molecules as a result of the absorption of laser

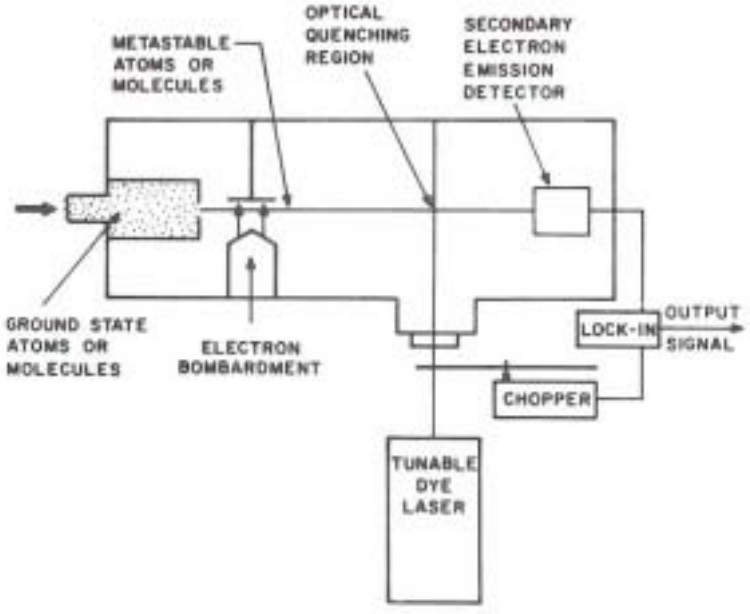

Fig. 15. Right-angle-interaction molecular beam spectrometer (from Ref. 24).

light. The metastables are collected by a secondary emission detector. This detection scheme turns out to be much more sensitive than direct detection of the light absorption, in the sense that it can use a much smaller sample of atoms or molecules. Figure 16 shows a spectrum of the hydrogen molecule showing two sharp transitions whose width is 20 to 30 MHz. By comparison, the full Doppler broadening would be over 3000 MHz. Thus the experimenters have reduced the linewidth by a factor exceeding 100. The reason this is better than the saturation spectroscopic results shown earlier is the freedom from power and collision broadening which the use of an atomic beam and a linear interaction method allows.

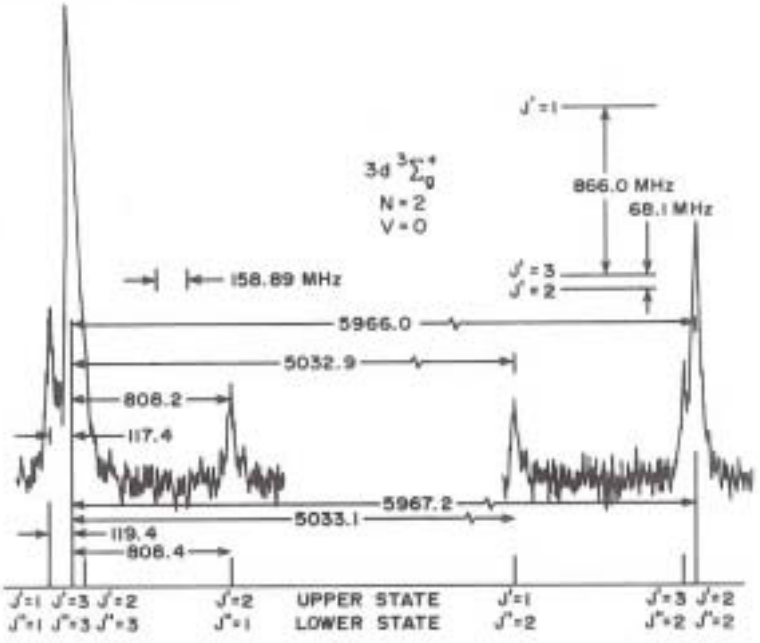

Fig. 16. Right-angle-interaction spectrum of molecular hydrogen (from Ref. 24).

To measure absolute transition wavelengths accurately, a careful calibration is required. Figure 17 shows the system used by Lichten and co-workers. The wavelength of the dye laser driving the transition is referred through a series of intermediate Fabry-Perot resonances to certain well-measured lines in the neon atom spectrum. To avoid bias from unknown phase shifts at the Fabry-Perot mirrors, the "method of virtual mirrors" is used, in which the results of measurements at two or more different Fabry-Perot lengths are combined to eliminate the phase-shift uncertainty.

The most interesting experiment that has been done by this group was again done on the Hα line of hydrogen. Accurate measurements of the line components were used to calculate the Rydberg constant in hydrogen R_H from the relation

$$1/\lambda = R_H(1/n^2 - 1/n'^2) + \text{small corrections} , \qquad (17)$$

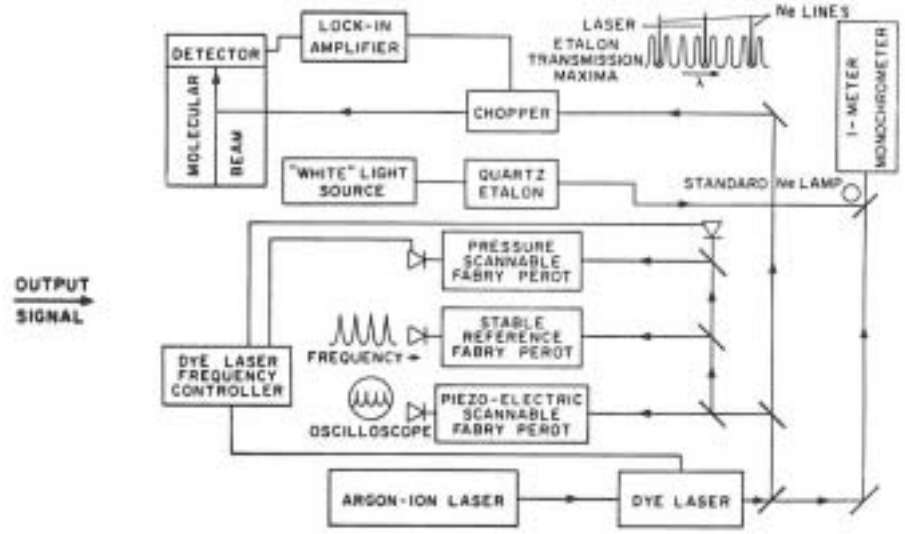

Fig. 17. Wavelength calibration system for right-angle-interaction spectroscopy (from Ref. 24).

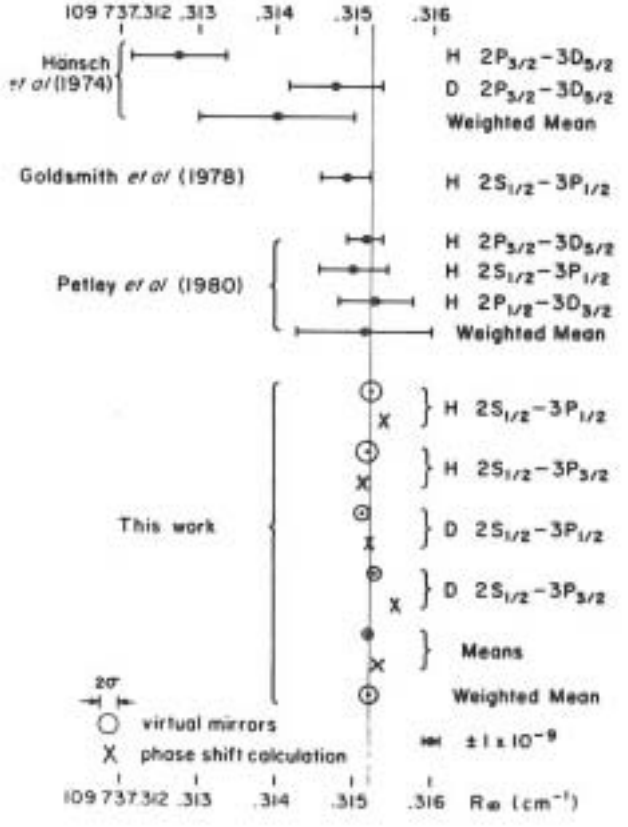

Fig. 18. Recent values of the Rydberg constant (from Ref. 24; see text).

where n=2 and n′=3. The first two terms come from the original Bohr theory. The small corrections come from relativity, quantum electrodynamics, and nuclear structure. Here Fig. 18 shows a number of recent values for the Rydberg constant in cm^{-1}. The "Hänsch et al." and "Goldsmith et al." results are both from the same Stanford group, using the saturation spectroscopic method described above. The "Petley et al." result is that of a group at the National Physical Laboratory in the U.K. "This work" is that of the Yale group. Not only is it the most accurate by far, but it reveals that the earlier work had some difficulties in error estimation. Evidently the Stanford group was too optimistic in stating its 68%-confidence error estimates, since only one out of four results overlap the much more accurate Yale value, whereas the NPL group was too pessimistic, since all three of its results hold to the Yale value excessively closely. It seems likely that the high quality of the Yale results was due more to careful experiment design and execution than to an inherently superior experimental method.

F. Doppler-free multiphoton spectroscopy

Multiphoton excitation of transitions offers another way to eliminate the Doppler effect. Figure 19 shows how this works. Suppose an atomic transition between states b and a is made by absorbing not one photon, in the normal way, but two or three, or perhaps even more, so that the total energies of all the photons absorbed add up to the energy difference between b and a. Let us calculate the frequency shift. Let ω_i be the frequency in the laboratory frame of the ith-absorbed photon and ω_i' be its frequency in the reference frame of the moving atom. Then the total energy absorbed by the moving atom, in frequency units, is

$$\omega' = \sum_i \omega_i' = \sum_i \frac{\omega_i - \mathbf{k}_i \cdot \mathbf{v}}{(1-v^2/c^2)^{1/2}} \,. \tag{18}$$

Now it is possible for $\Sigma \mathbf{k}_i \cdot \mathbf{v}$ to be 0 even if the individual $\mathbf{k}_i$ and the velocity $\mathbf{v}$ are not 0. The way to do this is to require that $\Sigma \mathbf{k}_i = 0$. In this case $\omega' = \omega$ to within an error which is of second order in v/c. To accomplish this in the case of a two-photon process, we must arrange the photons so that $\mathbf{k}_1 = -\mathbf{k}_2$: Their frequencies ω_1 and ω_2 are equal and their directions are opposed. In the case of three photons, if the frequencies are all equal, then their directions of propagation must lie in a plane $2\pi/3$ or 120° apart. If the frequencies are unequal then Doppler cancellation is still possible if the frequencies satisfy the triangle condition $\omega_1 + \omega_2 > \omega_3$ for any combination of frequencies. Both the two- and three-photon cases have been observed experimentally.[25,36] The transition strength may be quite weak compared to an allowed transition; however, if the light intensity is high enough, the rate of absorbing two photons or three photons may be enough that a signal can be seen.

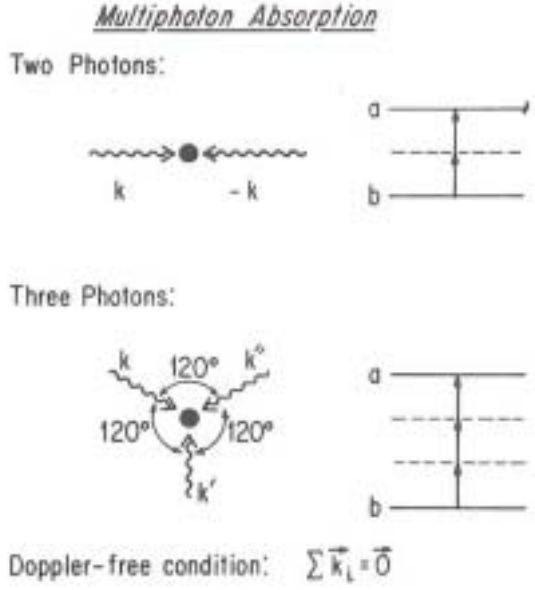

Fig. 19. Doppler-free multiphoton interaction geometries.

In practice, the two-photon experiments are usually done within a Fabry-Perot resonator; the standing optical field resolves into the two counterpropagating light beams. The resonance may be detected by one of several schemes, such as monitoring the fluorescent decay from the upper state a to a third state c.

Figure 20 is a sketch of a typical signal. One sees a very sharp resonance whose width is again given by the other broadening mechanisms

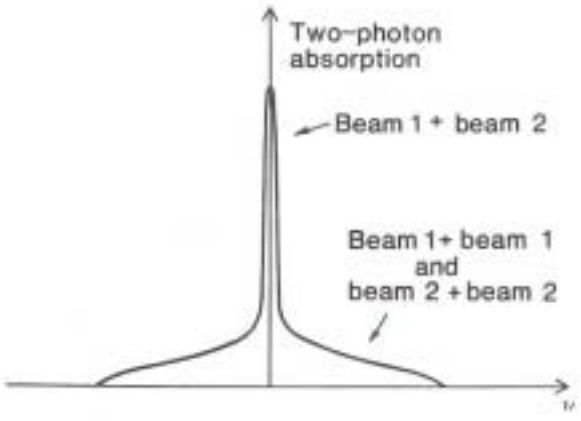

Fig. 20. Two-photon absorption spectrum in a standing light wave.

not including the Doppler effect. In addition, one sees a weak broad resonance, which comes from the atoms which have absorbed two photons from the same beam, so that the Doppler effect is not eliminated. The sharp resonance gives a very good indication of where the center of the line is.

An experiment of this type by Hänsch et al.[27] has yielded a very accurate value for the position of the ground state of hydrogen relative to n=2, which allowed a measurement the Lamb Shift difference between those states.

VII. TRANSIT BROADENING

At this point we have seen several techniques for eliminating Doppler broadening, the largest of the broadening effects listed in Table III. We have also seen that it is possible to eliminate the several effects that depend on pressure by operating in a low-density environment such as an atomic beam. It is appropriate now to take a short diversion and examine ways to reduce the "transit broadening." Once that is done we will turn to a recent technique which is capable of reducing all the above effects at once, namely trapped-particle spectroscopy.

A. Rabi resonance

As we saw earlier, if an atom interacts with a light beam for a time T, its transitions are broadened by the amount $\Delta\nu_T=1/2\pi T$. If T is the result of the motion of the atom through the light beam, this broadening is at root another velocity-broadening effect. This problem was first examined from the point of view of quantum mechanics by I. I. Rabi in 1937,[28] and has been discussed often in the literature. A two-level molecule interacts with a near-resonant sinusoidal perturbation that switches on at time t=0 and off at time t=T. T is much longer than the time required for the perturbation to induce a transition from the initial state |b> to the final state |a>. The amplitudes of states |a> and |b> are $C_a(0)=0$ and $C_b(0)=1$ at time t=0. The probability that the atom is in state |a> at time T works out to be

$$P_{ab}(t) = \left[\frac{(2b)^2}{(\omega-\omega_o)^2+(2b)^2}\right] \sin^2\{[(\omega-\omega_o)^2+(2b)^2]^{1/2}t/2\} . \qquad (19)$$

In these expressions, 2b is the matrix element of interaction between the field and the molecule, ω_o is the true transition frequency, and ω is the field oscillation frequency. The expression on the right side of Eq. (19) can be seen to be a product of a "Lorentzian" function and a function which oscillates at the frequency $\Omega_R/2$, where $\Omega_R=[(\omega-\omega_o)^2+(2b)^2]^{1/2}$ is the so-called Rabi oscillation frequency. The function P_{ab} for $T=\pi/2b$ is graphed as the dashed line in Fig. 21.

Often, in practical situations, not every atom will experience exactly the same length of pulse. For example, if one atom moves through the center of the beam and another atom moves through the side of the beam, the pulse length they experience will be different. Thus Eq. (19) must be averaged appropriately and the resonance shape is altered (solid curve). In addition, the intensities they experience will be different. If the distributions are is broad enough, averaging will convert the sine-squared function to 1/2, and the line shape will become

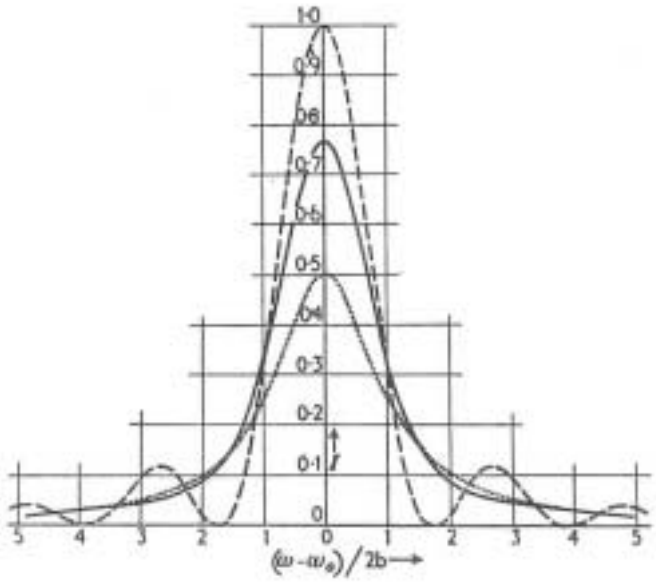

Fig. 21. Rabi resonance line shapes (from Ref. 29; see text).

a simple Lorentzian (dotted curve). This line shape is seen in many resonance experiments involving lasers, or molecular beams with radio-frequency fields as in Rabi's original situation, or nuclear magnetic resonance.

B. Separated oscillatory fields

In 1949 Norman Ramsey of Harvard University proposed[29] an improvement called the technique of separated oscillatory fields. This is the technique that is usually used now. Ramsey pointed out that an advantage is had if the interaction is broken up into two parts instead of one (Fig. 22). Usually the apparent frequency of interaction or the strength of the interaction is not precisely constant over the entire

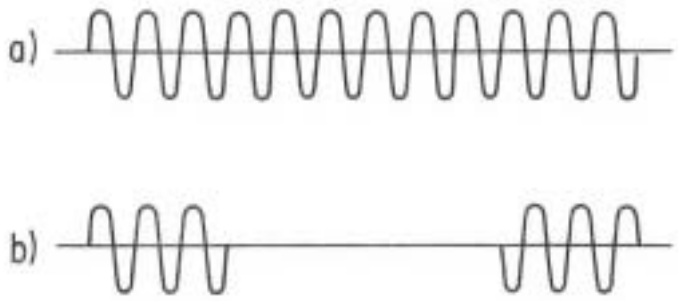

Fig. 22. Schematic waveforms of oscillatory atom-field interaction for (a) the single-field interaction technique; (b) the separated-field interaction technique.

time. For example, there may be a velocity change between the beginning

and the end of the interaction or an irregular Zeeman effect because of a stray magnetic field. The Rabi resonance would then be broadened. Ramsey observed that it is much easier to make, e.g., the magnetic field equal at two small separated regions, than over the entire long region. The transition amplitude is the product of two Rabi amplitudes with a time delay between them. All the complicated things which happen to the atom in the "dark" time between pulses can be subsumed into an overall phase and (conceivably) amplitude shift. The result of working out the theory is that the signal includes a broad resonance which comes from the interaction with one separated field, on top of which is a sharp oscillation representing the interference between the transitions induced by the two field pulses (Fig. 23). The shape of the sharp oscillation depends on the phase change between pulses. This line shape is very

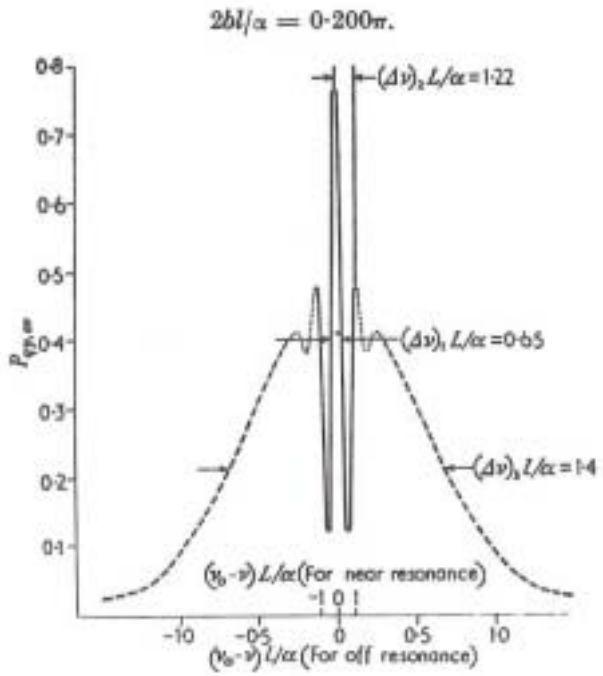

Fig. 23. Calculated separated oscillatory field resonance (from Ref. 29).

good for purposes of analysis of the exact line center. The sharp oscillation is also slightly narrower than the line shape produced by a single pulse of the same overall length. The reason is, loosely speaking, that the average width of the double pulse train is greater because there is none in the middle.

One of the nicest examples of the use of the separated oscillatory field method occurs in the cesium atomic beam frequency standard at the National Bureau of Standards in Boulder (Fig. 24). This is the primary frequency reference at present for the United States time scale. It consists of an atomic beam of cesium in which a transition between two hyperfine states is induced by separated fields in a microwave cavity made of two long pieces of waveguide with small holes for the beam to pass through.

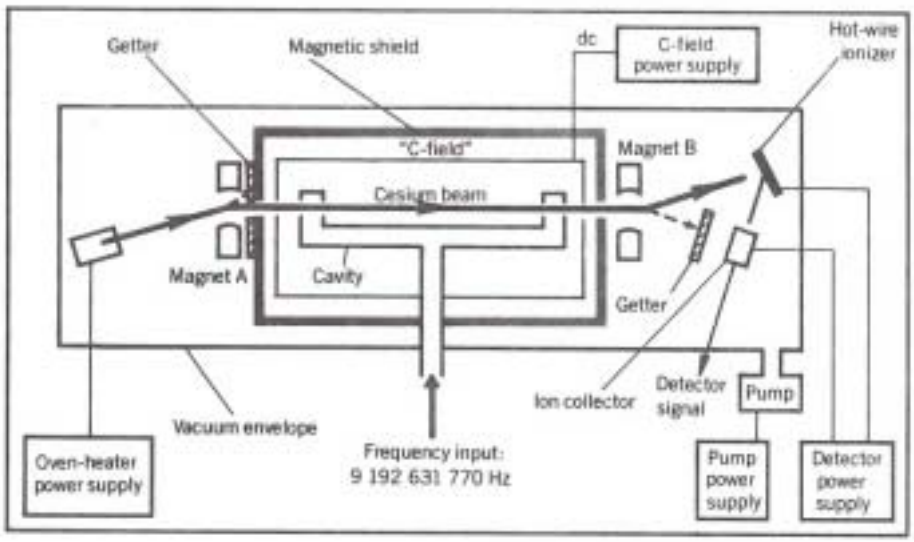

Fig. 24. Cesium atomic beam primary frequency reference (from Ref. 50).

The separated oscillatory field technique also has been applied many times in laser spectroscopy, using both two and three fields, and has yielded resonance linewidths for forbidden transitions at visible light frequencies as narrow as 650 Hz.[30]

VIII. ELIMINATION OF DOPPLER AND TRANSIT BROADENING BY CONFINEMENT OF PARTICLES

It should be clear already from the foregoing that much progress has been made in eliminating spectroscopic line broadening, and many beautiful techniques have been developed. The final technique for eliminating the Doppler effect is, I believe, superior to all of the others, and will ultimately yield the highest resolution in all of spectroscopy. This is the method of Doppler-free trapped particle spectroscopy. To see how this technique works, let us go back and look at the physics of the Doppler effect in more detail. To illustrate the point I wish to make it is sufficient to use a nonrelativistic approximation.

A. The role of photon momentum

Let us first see what conservation of energy has to say about the interaction of a photon with an atom (Fig. 25). The answer is very simple. If a photon of energy $\hbar\omega$ strikes a stationary atom of internal energy 0 and the latter is excited to a level of internal energy E, the energy conservation law says

$$\hbar\omega = E \, . \qquad (20)$$

Now suppose we treat a moving atom. The atom absorbs $\hbar\omega$, but its motion doesn't have any effect on its internal energy if we don't use special relativity. Therefore the atom's energy change is E just as before, Eq. (20) still holds, and there is no Doppler effect!

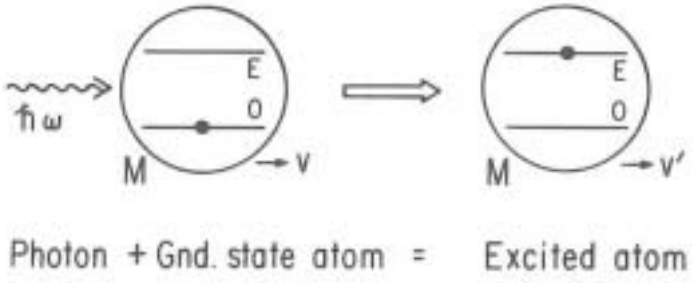

Fig. 25. Interaction of light with a free atom.

Now what have we left out? The answer is momentum conservation. Let us treat the problem again, including momentum as well as energy. The radiation has momentum $\hbar\omega\hat{k}/c$ per photon (this is actually a relativistic expression, but there is no nonrelativistic approximation for light propagation). The atom has kinetic energy $T_a=p_a^2/2M$. Its initial internal energy is again 0. Its initial momentum is $\mathbf{p}_a$. The atom's final momentum and energy are $\mathbf{p}_a'$ and $p_a'^2/2M + E$. Equating momentum before and after absorption yields

$$\hbar\omega\hat{k}/c + \mathbf{p}_a = \mathbf{p}_a' , \tag{21}$$

while energy conservation yields

$$\hbar\omega + p_a^2/2M = p_a'^2/2M + E . \tag{22}$$

Substituting (21) into the right-hand side of (22) and expanding yields

$$\hbar\omega + p_a^2/2M = (p_a^2 + 2\hbar\omega\mathbf{p}_a\cdot\hat{k}/c + \hbar^2\omega^2/c^2)/2M + E . \tag{23}$$

We may simplify this equation by cancelling identical terms on the left and right, dropping the term in ω^2, and rearranging. The approximation is permissible because $\hbar\omega/c<<p_a$, and therefore the ω^2 term is small compared to the one immediately preceding it. The error we make will be roughly of the same order of size as the errors made by neglecting special relativity. Using $\mathbf{p}=M\mathbf{v}$, we find

$$\omega = \frac{E/\hbar}{1+v_{ak}/c} = (E/\hbar)\,[1-v_{ak}/c+0(v^2)] . \tag{24}$$

Here v_{ak} is the component of the atom's velocity in the direction of light propagation. Neglecting the v^2 term on the right (in any event, it is probably incorrect because of our nonuse of special relativity) gives us the nonrelativistic expression of the Doppler shift of the spectral line.

B. Giving the photon momentum away: origins

We now have found that the Doppler effect is a result of the absorption of photon momentum by the atom, magnified by the atom's

velocity. This gives a clue to how we can eliminate the effect: we must find a way to make the atom absorb the photon energy but not the photon momentum. Therefore something else must absorb the photon momentum. There have been several suggestions about how to do this in recent years; the common idea is that a third body must be present to absorb the photon's momentum while the atom absorbs its energy. Thus the atom must interact with the third body, yet in order to allow close approximation of the situation of an isolated atom, the interaction must perturb the atom's internal structure as little as possible.

The first detailed treatment of this problem was given in 1937 by W. E. Lamb. In a paper[31] discussing the absorption of neutrons by hydrogenous substances, Lamb showed that if an atomic nucleus in a bulk object absorbs a neutron, the nucleus can absorb the momentum as well, in which case it gains some additional energy of motion, or else it can transfer the momentum to the lattice, and the entire bulk object can absorb the momentum, with the state of the relative motion of the absorbing nucleus and the bulk object left unchanged. Because the object is nearly infinite in mass compared to the nucleus, the second process involves very, very little change in velocity, and a sharp absorption line was predicted to result. He also showed that if the nucleus underwent a discrete change in motional state as a result of the absorption, discrete peaks or sidebands in the velocity spectrum of absorption would occur.

The conceptual roots of this problem go back much farther than 1937, at least to the beginning of the twentieth century with the discovery of Bragg scattering of x-rays by crystals. The Bragg problem is usually discussed in terms of the coherent constructive or destructive addition of scattering amplitudes from many lattice atoms, but it can be seen that the same basic phenomenon - the absorption of the atomic recoil by the entire crystal - can be viewed as responsible for the sharp angular scattering resonances. The Bragg problem is in turn closely related to the much older problem of the interaction of a light wave with a diffraction grating, but a discussion of it in terms of momentum conservation had to await the advent of at least the modern theory of electromagnetism and the notion of energy quantization. The first discussion of momentum conservation in light diffraction which I am aware of was given by Duane in the late 1920's,[32] who derived the angular resonant scattering from these principles.

In 1958 R. Mossbauer independently discovered that if gamma rays are absorbed by nuclei in crystalline substances (e.g., ^{57}Fe), then it is possible to obtain an extremely sharp absorption line from the same mechanism. Mossbauer spectroscopy[33] has become a very useful tool for studying crystal properties as well as properties of nuclei, because of the Lamb-Mossbauer sidebands which result from the lattice excitation. These can be detected via the Doppler effect by translating the entire crystal. The extreme sharpness ($\nu/\Delta\nu > 10^{11}$) of the Mossbauer line has also made possible fundamental physical measurements such as the Pound-Rebka measurement of the gravitational redshift.[34]

In 1953 R. H. Dicke[35] discussed the theory of absorption of a photon by an atom which was in the presence of many other atoms, in a so-called buffer gas, as in the field of optical pumping. He also gave a discussion of the absorption in case the atom was inside a box having

rigid walls. In either case, the momentum of the photon was given up to the other atoms with which it was constantly colliding, either in the gas or in the box walls. This phenomenon occurs in microwave resonance spectroscopy in a waveguide or cavity, and probably was present in microwave spectra for many years before it was described theoretically or noticed experimentally.

The multiphoton Doppler-free absorption described earlier is an example of essentially the same momentum-transferring phenomenon, with the radiation field itself playing the role of the third, momentum-absorbing, body. An analogous phenomenon is the line narrowing that results from the elimination of inhomogeneous magnetic-field broadening in rotating-sample nuclear magnetic resonance. The rapid passage through the range of applied field values causes all the nuclei to participate in the resonance at once.

C. Example: the hydrogen storage-box maser

One of the nicest examples in the microwave regime is the atomic hydrogen maser (Fig. 26).[36] Atomic hydrogen in the ground $1^2S_{1/2}$ state has two hyperfine levels whose total angular momenta are F=0 (lower)

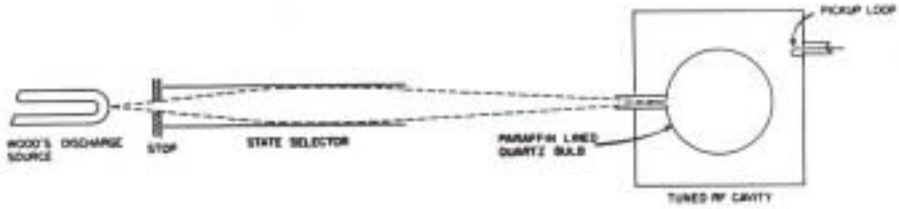

Fig. 26. Interaction of light with a free atom.

and F=1 (upper). The F=1 to 0 transition frequency is approximately 1420 Mhz; this is the same line that is well known in radio astronomy. The hydrogen atoms pass through a state selector which focuses the atoms in the upper state into a small hole in a round box whose inner walls are teflon-coated. The atoms in the lower state are defocused, and most of them don't go through the hole. Therefore the hyperfine population in the box is inverted. To make a maser, the box is enclosed in a microwave cavity tuned to 1420 MHz and a small amount of resonant radiation is coupled in or out with a pickup loop. Above a certain incident atom flux the maser breaks into self-sustained oscillation. Below the threshold flux it can act as a highly selective, low-noise amplifier of 1420 MHz radiation.

What happens to a hydrogen atom when it passes through the hole? In a short time it hits the wall, and then it bounces in some direction, and then it hits the wall again and bounces again, and again, perhaps several thousand times, before ultimately finding its way back out the hole. The atoms may be stored in the box for a period of on the order of one second. And since the microwave cavity's dimensions are on the order of the wavelength of the transition, the entire complicated bouncing motion takes place within a single wavelength of the radiation that the atom is absorbing or emitting. As we will see below, this satisfies the criterion for efficiently transfering the momentum of the photons to the walls. The maser line is therefore Doppler-free and

extremely sharp, and in fact the hydrogen maser is among the most precise frequency sources at present. The resonance linebreadth is given by the reciprocal of the storage time and may be 1 Hz or less. The center of the line is reproducible to better than a thousandth of a hertz. The frequency is on the order of 10^9 Hz, and so the precision can exceed 10^{12}, and actually approaches 10^{14} to 10^{15} in precisely built devices.

Despite such precision, the hydrogen maser is not used for the U.S. time standard. Each time the atom hits the wall, the relative quantum mechanical phase of the upper state and the lower state wave functions shifts slightly. The accumulating phase shift produces a frequency offset which is not well understood, because the interaction of the atom and the wall is very complicated; but more seriously, it depends on the nature of the wall surface (fluorocarbons, a water film, vacuum pump oil, and molecular hydrogen), which ages. As a result, the long-term stability is inferior to that of the less precise cesium beam clock, which is the present time standard reference.

4. Underlying principle of recoilless absorption

The central question in understanding these phenomena is "under what conditions will the atom be likely to give away the photon's momentum to the other objects it is in contact with, and under what

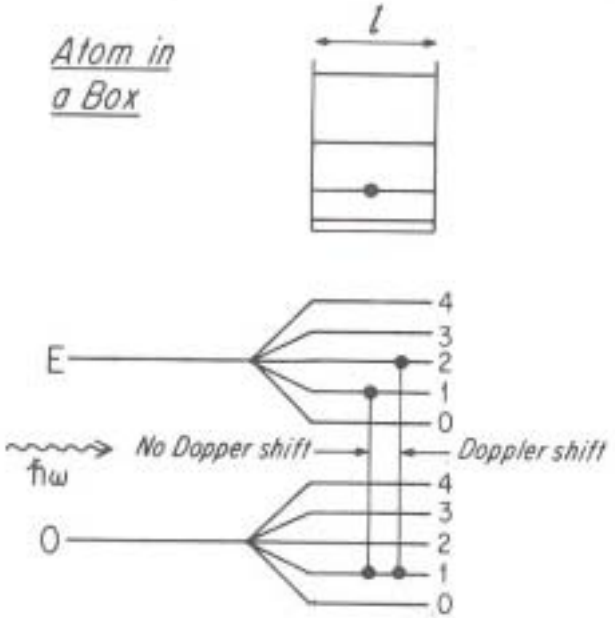

Fig. 27. Interaction of light with a confined atom.

conditions will it keep the momentum to itself?" When it keeps the momentum, the absorption line will have a broad Doppler spectrum; when it gives the momentum away, the absorption line will show no ordinary Doppler broadening, as in the derivation of Eq. (20) when momentum conservation was neglected. To provide an answer, let us look at Fig. 27. An atom is confined in a one-dimensional box which we represent by a square potential well. The total of the atom's internal energy and energy of motion is now quantized, and since the internal energy is

quantized as well, the motional energy has values given by the eigenstates of a particle in a square well. Now let us shine light on the atom. Its internal energy states $E_b=0$ and $E_a=E$ each have a fine structure given by the energy spectrum of the atom's motion in the box. If the atom starts out in a certain motional energy sublevel of E_b, and after absorption ends up in the same motional sublevel of E_a, then its momentum change is zero and there is no Doppler shift in the spectral line. If while it absorbs light it also changes its motional state, there is a nonzero Doppler shift. Another way to think about the situation is shown in Fig. 28. The moving atom absorbs the photon, its state of motion changes, it then strikes the wall, and its state of motion changes

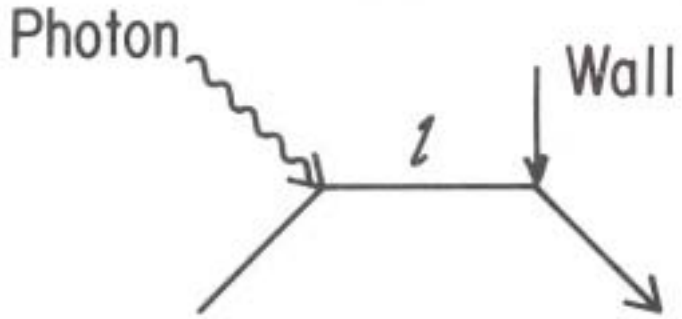

Fig. 28. Interaction diagram for transfer of photon momentum to wall.

again. If the momentum of the photon is absorbed by the box, then the final motional state of this process must be indistinguishable from that of the process where the atom only interacts with the wall. The uncertainty principle then gives the condition that makes it probable for the atom to give the momentum to the box without changing its own state of motion. The uncertainty Δp_a in the atom's momentum times the uncertainty Δx_a in its position is greater than or equal to $\hbar$. Δx_a is about equal to ℓ, the size of the box. This means that Δp_a is about equal to $\hbar/\ell$. For the above-mentioned indistinguishability to hold, the uncertainty in the atom's momentum must be greater than the momentum it transfers, the photon momentum, which is $\hbar\omega/c=\hbar/\lambda\!\!\!^{-}$, where $\lambda\!\!\!^{-}=\lambda/2\pi$. Thus

$$\hbar/\ell \geq \hbar/\lambda\!\!\!^{-}, \text{ or } \ell \leq \lambda\!\!\!^{-} . \tag{25}$$

When this condition holds true, the atom will be likely to return to the same state of motion after it absorbs light and hits the wall. When this condition does not hold, the absorption and hitting the wall probably will be independent events, and the atom will be likely to return to a different final state of motion. Then there will be a Doppler effect.

Figure 29 shows a sketch of the absorption spectrum of an atom in a box. When the box is much larger than the wavelength of the light (upper curve) the absorption spectrum has many lines. The envelope of absorption intensity is closely similar to the one-dimensional Maxwell-Boltzmann velocity distribution of Fig. 5. However, if the box dimension is comparable to $\lambda\!\!\!^{-}$, then there are only a few absorption lines spaced far apart (lower curve). The center line, where the momentum is all given to the box, is normally the most intense. If one can resolve this

center line, then one has achieved Doppler-free spectroscopy.

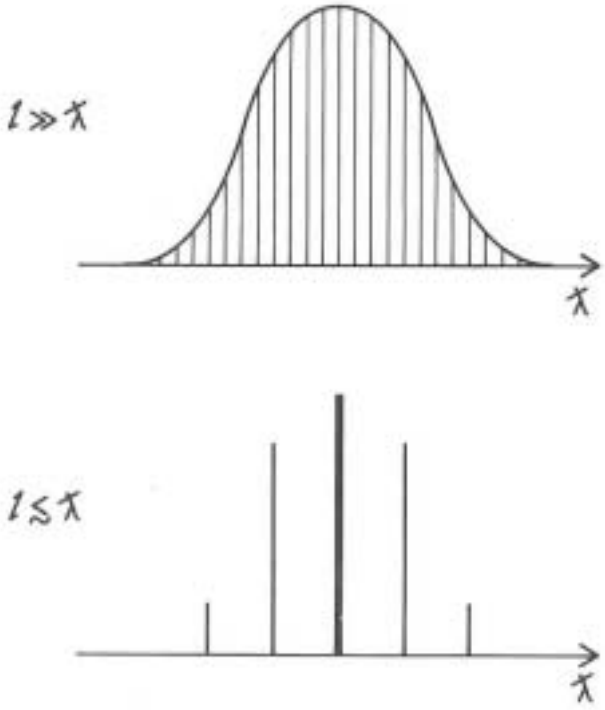

Fig. 29. Absorption spectrum for light of angular wavelength λ by an atom confined within a dimension l.

E. Confined particle spectroscopy

Now let us look at the ultimate scheme to eliminate the Doppler broadening in spectroscopy, by giving the momentum to the walls. This ultimate way so far can only be applied to charged particles, that is to say, ions and individual electrons. It consists of storing the particles in a stationary limited volume of space by applying carefully chosen electric and magnetic fields to keep them from moving away from the volume - namely, by storing them in an electromagnetic trap.

1. Trap principles

There are several types of traps; the two most important ones for spectroscopy are the radio-frequency trap and the Penning trap. The radio-frequency trap consists of two end caps at the same potential and a ring electrode biased relative to them. The electric potential near the origin has the form

$$\phi(r,t) = (V_{dc}+V_{ac}\cos\Omega t)(x^2+y^2-2z^2)/r_o^2 . \qquad (26)$$

Consider a positive particle in the trap. When the voltage factor in Eq. (26) is positive, the particle is attracted axially to the nearer end cap, away from the ring midplane, and is repelled radially from the ring toward the caps axis. When the potential reverses, so do the forces. As the potential oscillates the particle is alternately pulled this way and that; if the oscillation is rapid enough, and the voltages V_{dc} and V_{ac} are suitably chosen, the net result is that it will stay in the middle.

The theory of the confinement process stems from the theory of Mathieu functions. These same functions appear in the motion of satellites in the combined field of the earth and moon, or the motion of the moon in the combined field of the earth and the sun. The atom obeys a differential equation of motion which is similar to that for a mass attached to a spring, when the spring has a time-dependent oscillatory restoring constant.

The Penning trap (Fig. 30) has the same electrode structure as the radio-frequency quadrupole trap. In place of the radio-frequency drive voltage, a magnetic field is applied along the axis. A constant bias potential is applied between the two end caps and the ring. The charged particles are confined to trajectories which spiral about the magnetic field (z axis); their excursions in the z direction are limited by repulsion from the end caps. Again confinement results. Additional small ac fields may be applied at various points to drive the particles' motional resonances.

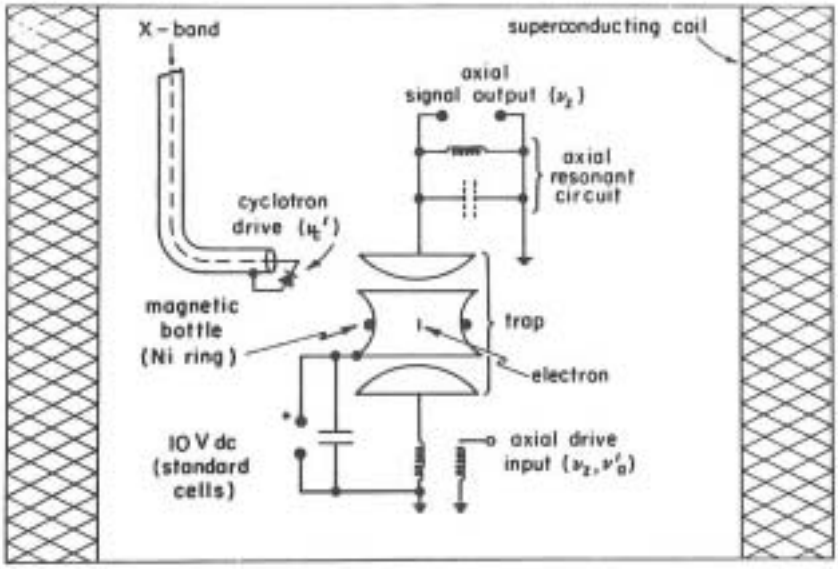

Fig. 30. Penning trap for electrons (from Ref. 37).

Spectroscopy can now be performed on the confined particles, either on internal structure transitions if ions are being studied, or on magnetic-field orbital and spin flip transitions in the case of electrons (Fig. 30 shows an electron g-factor experiment). If the wavelength of the radiation is greater than the dimensions of the particle orbits, we can expect that when the particles absorb the radiation, they will do so without showing Doppler broadening. Figure 31 shows an example of such a transition in the $^{171}Yb^{+}$ ion, observed by Blatt et al.[51] at the University of Mainz, West Germany. The transition is between ground state hyperfine levels. The resonance trace is fairly noisy. Nonetheless, the resonance width is only 6×10^{-2} Hz whereas the center frequency is 12×10^{9} Hz. Therefore the ratio of the linewidth to the frequency is about 5×10^{-12}, and the resolution is extremely high. By comparison, the Doppler broadening we calculated for a typical

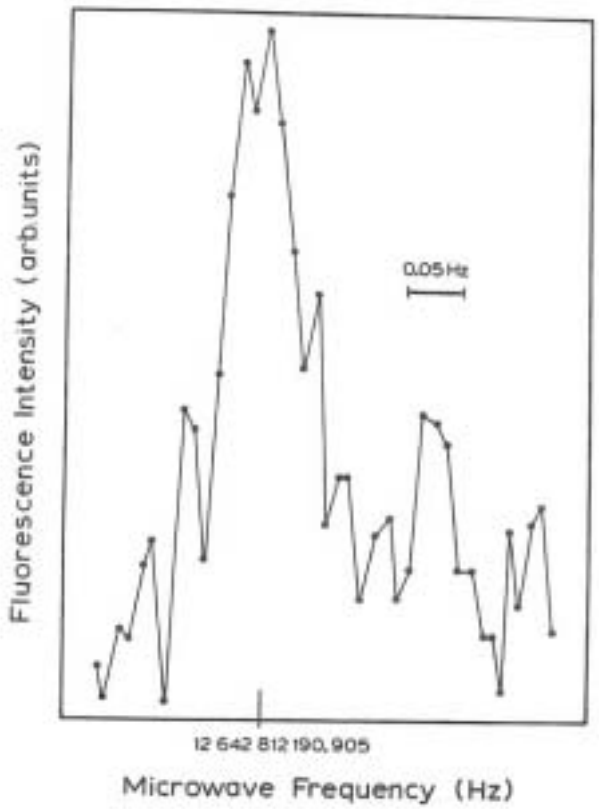

Fig. 31. Hyperfine resonance in trapped $^{171}Yb^{+}$ ions (from Ref. 51).

spectroscopic situation [Table III] was about 10^{-6} times the transition frequency. The resolution in Fig. 31 is 5 to 6 orders of magnitude greater: The line has been sharpened enormously by the process of transferring the momentum to the apparatus, and also somewhat further by the choice of a high-mass ion.

2. Limitations: confinement radius and second-order Doppler broadening

What are the limitations of this technique? There are two. First, if we want to go to higher and higher frequencies (for example, into the visible region), then the wavelength gets smaller and smaller and we must be able to confine the ions in a smaller and smaller volume to induce the momentum-transfer trick. Second, the momentum-transfer trick, like all the Doppler-free tricks we have studied so far, eliminates the Doppler broadening only to first order. There is still a residual velocity dependence of the transition frequency through the $(1-v^2/c^2)^{1/2}$ denominator in Eq. (13). If we expand this factor in a Taylor's series about $v=0$, we see that the range of frequencies will be about equal to v^2/c^2, or about 10^{-12} if $v/c\simeq 10^{-6}$. This effect is called second-order Doppler broadening. The only ways to reduce it are to make the atom move more slowly by cooling the motion or by changing to a heavier atom. Cooling the motion has the additional effect of making the particle's orbit smaller; this can readily be visualized if one imagines that the atom is moving in some sort of parabolic potential well. That,

in turn, will permit use of the momentum-transfer trick at shorter wavelengths. Increasing the particle's mass at constant temperature, however, does not shrink the orbit.

3. Cooling

To cool the motional temperature of the particles in the trap, we must put them in thermal contact with a lower-temperature heat reservoir. Several schemes to do this have been devised. The most straightforward is to admit a cold neutral gas, such as helium, to the trap. This is often done in the early stages of cooling, and the gas is subsequently pumped away.

Another scheme is electrical cooling (Fig. 32). A charged particle oscillating back and forth in the trap will induce an image charge of opposite sign to itself whenever it approaches an electrode. If an external wire connects the electrodes to a charge reservoir or another

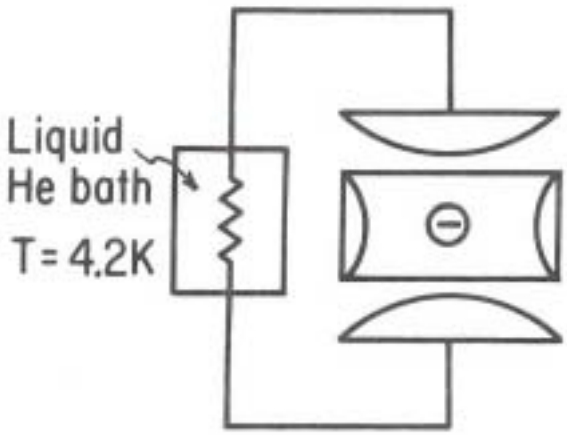

Fig. 32. Resistive cooling of electrically trapped particles.

electrode, a small oscillating current will flow. Thus, to cool the motion we can insert a resistor in the circuit to dissipate the electrical energy, which will damp the motion of the charged particle. The particle then gets "cold" as the resistor gets hot. Ultimately the two will come into thermal equilibrium and cooling will cease. The reverse energy flow mechanism that makes equilibrium possible is the thermal, or Johnson, noise voltage fluctuation between the resistor terminals, which always appears if the resistor temperature is greater than absolute zero. This fluctuating voltage is applied between the end caps and produces an oscillatory force on the electron which, on the average, increases its velocity. The resistor must be put in as cold a place as possible to achieve maximum cooling; typically this is a bath of liquid helium at 4 K or perhaps less (of course, the resistor must not become superconducting). The practical limit of this mechanism may be a few tenths of a kelvin.

A mechanism that does not work for elementary particles, but does work for particles that can absorb light, such as ions, is optical sideband cooling. To see how it works, let us return to the spectrum of

the absorption of an atom in a trap (Fig. 33). Let us shine light on the atom and drive a transition between the lower state and the upper state, not at the center frequency, but at one of the lower-frequency of the sidebands into which the Doppler-broadened profile has coalesced. If the

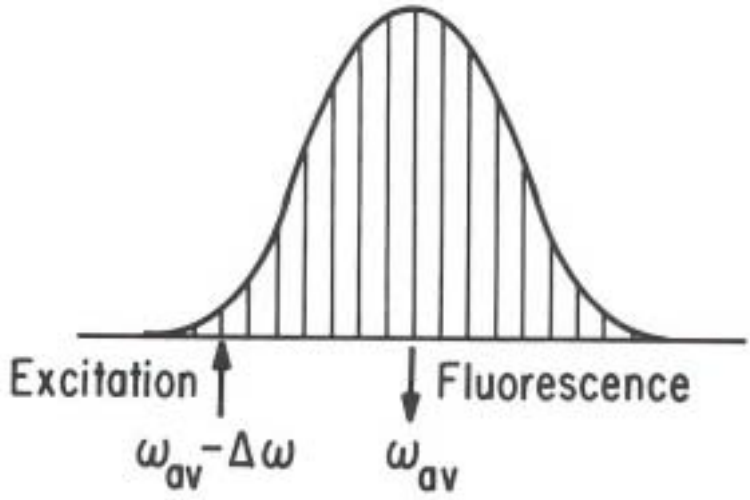

Fig. 33. Transition cycle in optical sideband cooling.

atom absorbs the light, eventually it will fluoresce or reradiate light. The absorption and spontaneous fluorescence are independent processes, so that the frequency which the atom emits need not be the same as that which it absorbs. In fact, the frequency that it emits may be anywhere in the atom + trap spectrum. Similarly, if the atom were freely moving in a gas, it might absorb the light from one direction and emit into another, therefore with a different Doppler shift $\mathbf{k}\cdot\mathbf{v}$; or it might hit something and change its velocity between absorbing and emitting. In each case, on the average it will emit at the center of the spectrum, and therefore on the average it will emit a higher frequency than it absorbs. The net energy added to the radiation field by the absorption-emission cycle is $\hbar\Delta\omega>0$. The source of the energy change must be an equal negative change in the kinetic energy of motion of the atom, since the atom's internal energy stays the same; the coupling mechanism is the recoil upon absorption and emission. The process can be visualized in terms of the trap-induced substructure of the ground state and the excited state; the net result then is a decrease in the motional quantum level. The amount of energy that can be extracted in one cycle of this process is a very small part of the total thermal energy, but since at the end the atom is again in the ground state, the process may be repeated, and after many cycles can extract almost all the kinetic energy from the system. Temperatures as low as 10 mK have been reached.[38] At 10 mK less than one part in 10^4 of the initial kinetic energy remains. This means also that the second-order Doppler effect has been reduced by a factor exceeding 10^4, and the amplitude of the atomic motion has been reduced by a factor of 10^2. Thus the goal of reducing the amplitude of the atom's motion to one wavelength of visible light is approaching; at this point[38] the radius of motion was less than 1 μm in the best case.

This trapping and cooling technique has another very great advantage, which is that it naturally permits very long interaction times. In principle, the atom can stay in the trap forever, so the time of interaction of the light and the atom can be as long as one wishes. Ultimately, the interaction time will be limited by some process that makes the interaction between the radiation and the atom lose coherence, such as a collision or spontaneous emission.

The ideal atom for optical sideband cooling and spectroscopy would have one state that decayed very rapidly to allow rapid optical pumping and cooling and another state that lived a very long time. Spectroscopy on the second state could be done with extremely high resolution. This is the goal of groups at the National Bureau of Standards in Boulder, Colorado, the University of Washington, the University of Hamburg, and a few other places around the world, as they seek to produce the ultimate line narrowing in spectroscopy.

4. Universal trapped particle refrigerator

There is a further small variation of the laser cooling process. There are particles that cannot be cooled by means of direct laser optical sideband pumping; for example, an elementary particle which has no internal states. Is it nevertheless possible to cool an elementary particle with laser cooling? The answer appears to be yes, although it has not been directly demonstrated. Suppose we put in a trap not one but two particles, one being the elementary particle we wish to study, and the other being an atomic ion such as Mg^+ or Ba^+ whose energy levels are conducive to optical sideband cooling. As the ion is being cooled, the elementary particle collides with it; the forces they exert on each other are Coulombic and hence very strong. Thus momentum will be transferred very rapidly from one to the other, they will thermalize, and the optical sideband pumping on the ion alone will cool both particles to approximately the same temperature. The final temperature should be slightly higher than before, since the heating mechanisms of the trap affect both particles while only one is cooled. An estimate shows that for any reasonable trap dimension, the coupling is quite strong enough. This "transference cooling" has been seen[39] in the spectrum of trapped Mg^+ ions (Fig. 34). The three transitions shown come from the $^{24}Mg^+$, $^{25}Mg^+$, and $^{26}Mg^+$ isotopes. The point to notice is that the linebreadth (predominantly the Doppler breadth) of each of the three lines is exactly the same. Yet the laser pumping was applied only to $^{24}Mg^+$, the most common isotope. Evidently Coulomb collisions equilibrated the temperatures of the three species very effectively. It seems likely that the method will also work well enough with very small numbers of particles, and with particles of different mass. Thus we will have produced a universal trapped particle refrigerator.

5. Ultimate sample size

To avoid collisions, one should work with as small a sample as possible. How small can this be? The answer is that it is possible to study spectroscopically a sample that contains only <u>one</u> ion! Figure 35 shows[40] the fluorescence intensity from a sample of trapped $^{24}Mg^+$ ions as a function of time. Periodically a charge exchange collision will

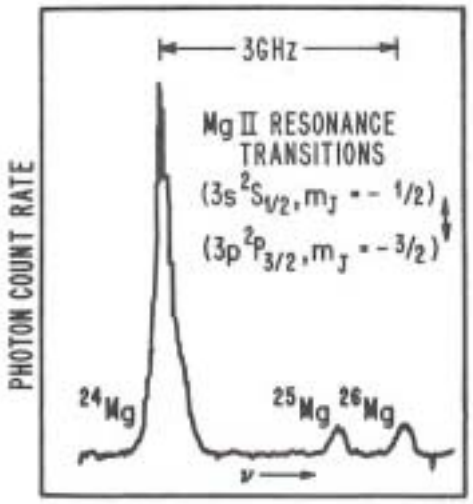

Fig. 34. Optical transitions in optically cooled Mg^+ isotopes (from Ref. 40).

occur between a $^{24}Mg^+$ ion and a ^{25}Mg atom from an atomic beam passed through the trap. Thus the number of $^{24}Mg^+$ ions decreases by one. When the decrease occurs, there is a sudden downward jump in the fluorescence intensity. If there were a large number of ions contained in the trap, the composite signal would average out to a smooth exponential decay. In Fig. 35, however, the sudden downward jumps are clearly visible, and it is evident that the number of ions in the trap decreases progressively from three, to two, to one, to zero.

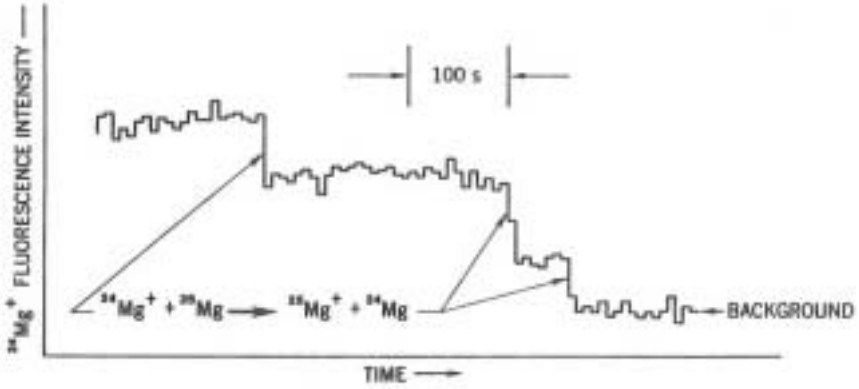

Fig. 35. Fluorescence from a cloud of trapped $^{24}Mg^+$ decaying from 3 to 0 ions (from Ref. 37).

A simple calculation verifies that it is possible to detect optically a single trapped ion. The lifetime of a typical excited state is about 10^{-7} sec. This means that if we pump the transition with laser light as hard as we please, the atom can radiate about 10^7 photons each second, since the probability that the atom is in the excited state can be made at most of order unity (actually about 0.5). If we catch even 1/1000th of the fluorescence with a photomultiplier, we are then

catching 10^4 photons per second from one single atomic ion. And that gives quite a strong signal, since good photomultipliers have a noise level of only 1 or 2 photons per second and an efficiency of 0.1 or better. An even more dramatic experiment to show this level of sensitivity is possible. A group[41] led by H. Dehmelt and P. Toschek made a very small radio-frequency ion trap employing optical sideband cooling and studied it with a microscope to which a camera was attached. They observed a small glowing spot of light (Fig. 36). As they reduced the number of ions in the trap and continued to take photographs, they found discrete steps in the fluorescent spot size, with no intermediate cases, and obtained photographs of spots consisting of three, two, and one ions.

Fig. 36. (Right side) photograph of fluorescing clouds of 3, 2, and 1 trapped Ba^+ ions; (left side) general view of fluorescence from trap; (insert) trap detail (from Ref. 41).

IX. REDUCTION OF RADIATION BROADENING

We have seen how to eliminate many of the physical effects which limit the precision in traditional forms of spectroscopy. Let us finally turn our attention to the radiation field. The major radiation effects are:

(1) Power broadening and shifts induced by the exciting light source
(2) Broadening and shifts induced by blackbody radiation
(3) Spontaneous emission broadening.

Power broadening by the radiation source can be an inherent problem only when the spectral line is detected in the radiation itself. This is the case because every radiation detector has a lower sensitivity limit; thus the applied radiation field intensity cannot be reduced indefinitely in the attempt to eliminate power broadening, for ultimately the signal will become undetectably weak. In practice this will be a problem only when other broadening effects have been reduced to very low values.

If a non-radiative detection method is employed, this restriction is removed. Detection of the atom in the excited state can, in principle, be sensitive at the single-event level. Some such methods, e.g., state selective ionization or collisions, have been very successful and can be carried far. However, the detection normally will destroy the level. Is it possible to do better than that? One suggestion might be to "weigh" the atom, taking advantage of the relativistic mass dependence on internal energy to ascertain which state the atom is in. It may be possible to accomplish the weighing with adequate precision by monitoring a motional oscillation frequency of the atom in a trap[62] since these frequencies are mass dependent. The extent to which this scheme of "quantum nondemolition" spectroscopy can be successful in principal appears to involve basic questions of quantum mechanics, thermodynamics, and information theory.

The blackbody radiation field has two effects. In first order it induces transitions from one state to another, thereby shortening the lifetime. In second order, it causes energy level shifts which can be modeled as dynamic Stark effects.[10] Figure 37 shows the blackbody-induced transition rates from principal quantum state n to all other states in the hydrogen atom at room temperature, and Fig. 38 shows the dynamic Stark shift of state n in the same conditions. The approximate models are due to Gallagher and Cooke,[9] and the exact calculations are due to Farley and Wing.[10] A hydrogen atom in the n=10 state will absorb a blackbody photon about 35,000 times per second. The dynamic Stark shift is on the order of 1 kHz for this state. Both of these effects can be reduced by lowering the temperature.

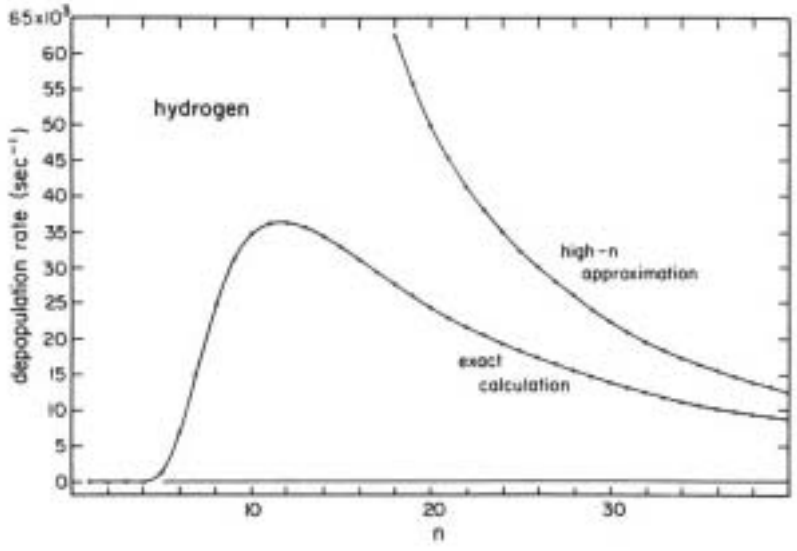

Fig. 37. Depopulation rate of atomic hydrogen states induced by 300 K blackbody radiation (from Ref. 10).

But how can we eliminate the effects of spontaneous emission? It seems as if it is an inherent property of the atom. However, that is not

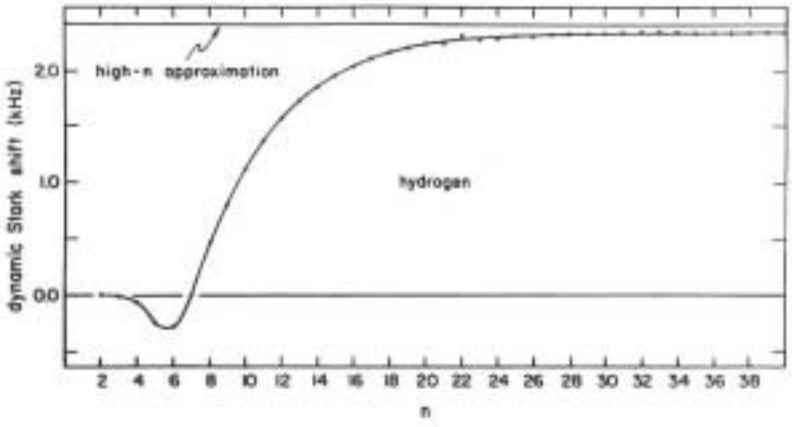

Fig. 38. Energy shift of atomic hydrogen states induced by 300 K blackbody radiation (from Ref. 10).

precisely true. When we solve Schrödinger's Equation for the energy levels of an atom, the levels we obtain have infinite lifetime. Why is it then that real atoms decay if they are in an excited state? The answer is that real atoms interact with virtual quanta in the radiation field even at absolute zero temperature. The many oscillatory modes of the radiation field contain no photons at absolute zero, but they still can receive photons. Because of the coupling between the atom and the field, after some time it will emit its energy into one of them. If we could eliminate the radiation field modes in the neighborhood of the atom, it appears plausible that we would eliminate the spontaneous emission. To do that we again must put the atom in a closed cavity, so that the distribution of radiation field modes as a function of frequency is discrete rather than continuous, and adjust the cavity dimensions so that there are no modes having frequencies near those which the atom is likely to emit. For microwave transitions this can be done by making the cavity dimensions less than roughly λ. For optical frequencies this cavity size is so small that it is impractical, but it may be possible to position the transition frequency in between cavity modes, if the cavity Q is high enough and the atomic transition is sharp enough that the relevant lines are all well resolved.

In this way the atom could be made to have a long lifetime. What would ultimately limit it? First, the atom might drift out of the cavity, or against a wall; this, however, could be eliminated if the atom were confined near the center electromagnetically. Second, if more than one atom were present, two or more might emit cooperatively to produce a photon having enough energy to match a cavity mode. Third, if the cavity temperature were greater than zero, a Raman process might occur in which the atom absorbed a photon from a lower-frequency mode and emitted one into a higher-frequency mode while de-exciting itself. Finally, it might de-excite by a nonradiative loss mechanism such as resistive heating of the cavity walls (if not superconducting at the transition frequency) by the fluctuating near field of the atom.

A step toward realizing this idea has been made by Vaidyanathan et al.[43] A beam of Rydberg atoms was sent not into a cavity, but into a

space between two parallel conducting plates. The space between such plates is not completely isolated from the outside space, yet it is partially isolated, so the density of radiation field modes is different inside than in free space. In particular, there is a cutoff frequency for one polarization of the oscillatory electric field, below which the mode density vanishes. A dc electric field was used to tune (via the Stark effect) the frequency of one of the transitions out of the initially excited state across the cutoff frequency of the "cavity." Their result is shown in Fig. 39. As they adjusted the frequency, they found an increase in the depopulation rate of the atom that occurred when the 29d-30p transition was tuned across the guide cutoff frequency (left curve). When the 28d-29p transition was tuned over the same Stark field range, it did not cross the cutoff frequency, and no jump was seen (right curve)

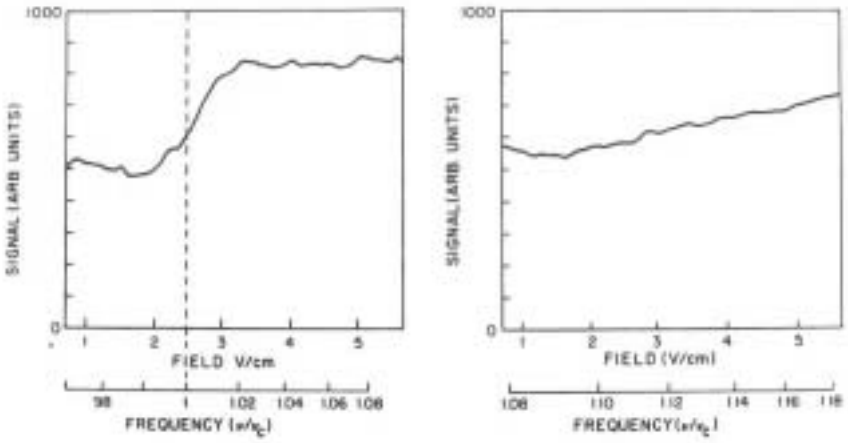

Fig. 39. Evidence for modification of the blackbody field spectral distribution by a resonant structure (from Ref. 43).

It should be emphasized that under their conditions (T=180 K), each mode contained many photons, and hence their results are due to blackbody radiation rather than to virtual radiation. Nonetheless, the idea of modifying lifetimes by changing the mode structure of the space surrounding the atom has been successfully demonstrated, and it will be interesting to see whether it works also for virtual radiation. Presumably, accompanying the shutoff of spontaneous decay will be a modification of the level shift which results from the coupling to the radiation field.

X. SPECTROSCOPIC SOURCES AND INSTRUMENTS

The final major topic to be discussed is the limits to precision of spectroscopic light sources and instruments.

A. The electromagnetic spectrum of spectroscopy

Figure 40 indicates the range of devices needed to cover the portion of the electromagnetic spectrum that is of greatest interest for spectroscopy of transition frequencies in atoms and molecules, lying between roughly 10^7 and 10^{16} Hz. Between 10^7 and about 10^{10} or 10^{11} Hz are found fine and hyperfine structure transitions in atoms, many Rydberg state transitions, and, in the upper part of the range, rotational

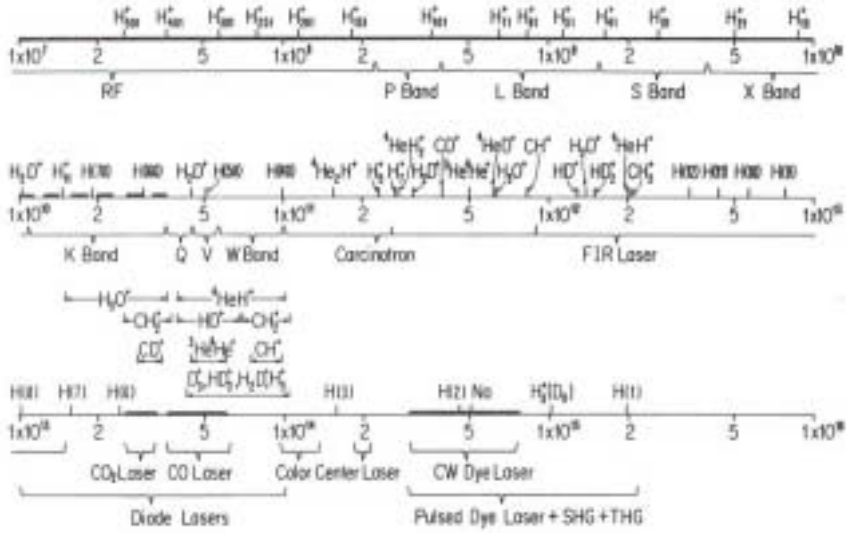

Fig. 40. Electromagnetic spectrum of interest in spectroscopy, with frequency ranges of certain interesting categories of transitions and types of coherent sources indicated. Notation: H(n) denotes the transition between principal states n+1 and n in atomic hydrogen; H_n^+ denotes the fundamental rotational frequency of a molecular ion containing n hydrogen atoms.

transitions in most molecules. In the range from about 10^{11} to 10^{12} Hz lie rotational transitions in light molecules, such as diatomic molecules in which one atom is hydrogen. In the range of roughly 10^{12} to 10^{14} Hz lie vibrational transitions in molecules, the hydrogen-bearing ones being near the upper end of the range. Low-lying electronic transitions in ordinary atoms and molecules lie in the region of roughly 10^{14} to 10^{16} Hz. Low-lying transitions in multiply ionized atoms lie in the region 10^{16} to 10^{19} Hz, off the diagram. Finally, nuclear x-ray transitions lie in the approximate range 10^{19} to 10^{22} Hz. I will not discuss the region above 10^{16} Hz, however, because up to the present, although some beginnings have been made, there has been comparatively little progress in the development of coherent sources there.

It can be seen from Fig. 40 that many different types of devices, based on many different technologies, are required to cover the frequency range of interest in high resolution spectroscopy. The underlying reason, of course, is that radiation-source technology draws from the same manifold of widely varied physical phenomena as do the samples of interest, and so naturally the technological details of the devices vary widely as well.

Generally speaking, the tuning band of an individual device increases less rapidly than does the center frequency of the band. Generally, also, the cost of individual devices increases as the frequency increases, since the dimensions of the active element shrink, and the technology becomes progressively more exotic. Accordingly, the cost of high resolution spectroscopy is quite high. In the centimeter and millimeter microwave bands (10^9-10^{11} Hz), the cost of a complete high resolution source may be in the range US \$3,000-10,000 per GHz of frequency coverage. In the visible region, the cost of a state-of-the-art cw dye laser system may be in the range of only US \$1-3 per GHz coverage. Nonetheless, even the minimum US \$1 figure implies a facility cost of US \$10 million for relatively complete coverage of the 10^7-10^{16} Hz range, and it is likely that the actual cost would be substantially more. At present there is no laboratory in the world which can claim to cover even a substantial fraction of this range with state-of-the-art equipment. The lack of such a facility is a major impediment to progress in high resolution spectroscopy.

B. Frequency measurement

The problem of calibrating the frequency is about as expensive to solve as is the problem of generating the frequency. There are two ways to determine the frequency of an oscillatory wave. One is to measure the frequency directly, and the other is to measure the wavelength and convert using the relation $\nu\lambda=c$. It might appear that these are equivalent. In fact, however, they are not only inequivalent but are sufficiently different as to have caused significant confusion in past years. The essential difficulty lies in the limited accuracy of the speed of light, which itself must be calculated from wavelength and frequency, or length and time interval, measurements.

Figure 41 summarizes measurements of the speed of light from 1675, the first successful measurement in recorded history, to the present. The scale changes several times, an indication of the remarkable increase in precision over the centuries. The accuracy at present is 1 part in 10^9. An interesting historical point, and a lesson for experimenters, can be learned by following the record backward in time from the present. Recent values agree reasonably well with each other within their accuracy estimates, the earlier ones being progressively less accurate, as would be expected. Suddenly, however, we come upon a series of results obtained from roughly 1930 to 1950 which are consistent with each other but inconsistent with the modern value, yet whose precision increased steadily as time went on. Most of these measurements were made in effect by measuring the propagation time of a light pulse along a reflecting circuit and back. They differ from the modern value by at

least two to five or more times their error bands. If the error bands are assumed to represent 1 standard deviation, or 68% probable, errors, the probability that a two-standard-deviation error arose by chance is about 5%. If the error bands represent a higher confidence level, the probability of a chance error is smaller still. The probability that the deviations of all of the experiments in this sequence arose by chance is quite clearly negligible.

Fig. 41. Values of the speed of light (from Ref. 48).

The origin of this phenomenon seems to be the 1928 Karolus and Mittelstaedt experiment, rapidly reinforced by the experiments by Michelson, Pease, and Pearson in 1931-32. The latter work was actually done largely by the two co-authors, since Michelson's health was failing, and he died before most of the data were taken. The Michelson apparatus consisted of a tube a mile in length, evacuated by many vacuum pumps. A light pulse was sent along it, reflected from a mirror at the far end, and the return pulse was detected. The speed of light was defined as twice the tube length divided by the round-trip propagation time. The technique was basically a scaling up of similar experiments that had been done for the previous 100 years. The work was the culmination of a long series of speed-of-light experiments by Michelson begun in 1880, whose result was that Michelson became famous and a figure of great

authority on the subject. It seems clear in retrospect that subsequent workers did not expect to find a serious disagreement with the value bearing his imprimatur. This appears to explain the fact that one after another got erroneous results conforming to Michelson, Pease, and Pearson's value, with progressively shrinking error bars.

Several reviewers have tried to ascertain the reasons for the series of mistakes. The review by Bergstrand[53] brings out two common elements in the later work through about 1950: (a) the authors, in Bergstrand's opinion, tended to underestimate systematic errors resulting from peculiarities of their apparatus or technique; and (b) the final result was the average of a very large number - typically 400 to 3000 - individual measurements. Random errors are those which vary in an uncorrelated way from run to run; systematic errors are the same over the entire data set, or large blocks of it. Averaging n readings reduces the random error in the result by a factor about equal to $\sqrt{n}$, or 20 to 55 in these experiments. A systematic error considerably smaller than the random error in a single measurement could nonetheless be considerably larger than the random error in the mean, and thus could bias the final answer. Unmasking the bias, however, would require either a subsidiary experiment of accuracy much higher than the individual measurement error, an unlikely possibility since the experimenters were presumably already working at the limit of their technical skill and apparatus quality; or else careful searching through the data for correlations with experimental conditions, which was apparently not done, and even if done is not always successful.

An explanation of the "locking" of each successive result to its predecessor has been given by R. T. Birge,[54] who attributed the thought to E. O. Lawrence:

> "In any highly precise experimental arrangement there are initially many instrumental difficulties that lead to numerical results far from the accepted value of the quantity being measured ... . Accordingly, the investigator searches for the source or sources of such errors, and continues searching until he gets a result close to the accepted value. Then he stops! ... In this way one can account for the close agreement of several different results and also for the possibility that all of them are in error by an unexpectedly large amount."

The locking presumably continued until an experimenter came along with such improved technique, or independence of mind, or both, that the sequence was broken (and perhaps a new one was initiated).

Regarding the source of the errors in the Michelson, Pease, and Pearson result, Cohen and Dumond[55] have pointed out the following defects of technique: that the co-workers made 2885 propagation time measurments, but only 2 or 3 distance measurements, presumably because the latter was much more tedious and difficult; that the former measurements were made at night, the latter during the day, leading to the possibility of, for example, a systematic unaccounted-for temperature shift; and that the results showed a correlation with the ocean tides

[the site was near Los Angeles, California] which was never satisfactorily explained.

Evidently an independent frame of mind and confidence in one's own skills are of crucial importance to an experimenter who follows in the footsteps of the past. In fact, the wisest thing such an experimenter can do is to resist calculating the final answer until the day after the experiment is over. If he or she is honest about not "peeking," this prevents him or her from knowing where he or she "wants" to go, and hence from drifting in that direction, whether unconsciously or by choice.

The advances in technology after the second world war made the error bars shrink so rapidly that the discrepancy in the Michelson result no longer could be overlooked. The most accurate measurements all are done now by measuring the frequency and the wavelength of the same oscillation and multiplying, rather than by pulse timing. The results of the two methods are not the same quantity in principle; the pulse timing method measures group velocity whereas the wavelength-frequency method measures phase velocity. However, the numerical difference vanishes in the absence of dispersion, and experiments at widely different frequencies have indicated that the physical vacuum has no detectable dispersion.

The most recent experiments in Fig. 41 measured the wavelength and frequency of an infrared methane-stabilized helium-neon laser transition. The wavelength measurement was made by interferometric comparison with the krypton length standard; the frequency was measured by heterodyne comparisons with a local frequency standard. The 1 part in 10^9 present accuracy is near the technical limit of precision of comparing lengths, and so it is impossible to make the speed of light very much more accurate. However, an alternative is to define the speed of light at the best present value and eliminate the length standard as a primary standard; time would then be primary, and length would be derived from it via c. It appears likely that this redefinition will be made at the October 1983 Conference General des Poids et Mesures, with the meter being defined as "the length of the path traveled by light in a vacuum during a time interval of 1/299,792,458 of a second."

The technology to measure the frequencies of oscillations in the higher portions of the band of Fig. 40 is just becoming available. Thus, in practice, one often uses wavelength technology in the visible and near-infrared regions even though it is not quite as precise as frequency technology. Figure 42 shows schematically the sort of device which is used to measure wavelengths.[44] In essence it is a scanning interferometer. As the length of the resonant section between the two corner cubes varies, a series of standing wave fringes are seen in the diode detector outputs for each of the two laser wavelengths traveling in the device. The ratio of the number of fringes for each laser line is equal to the ratio of the line wave numbers (the reciprocals of the wavelengths). Thus an unknown wavelength (of the dye laser) can be measured in terms of a known one (of the helium-neon laser). Stray phase shifts from wavefront irregularities, diffraction, uneven mirror displacement, and other causes, limit the comparison accuracy to about 1 part in 10^9.

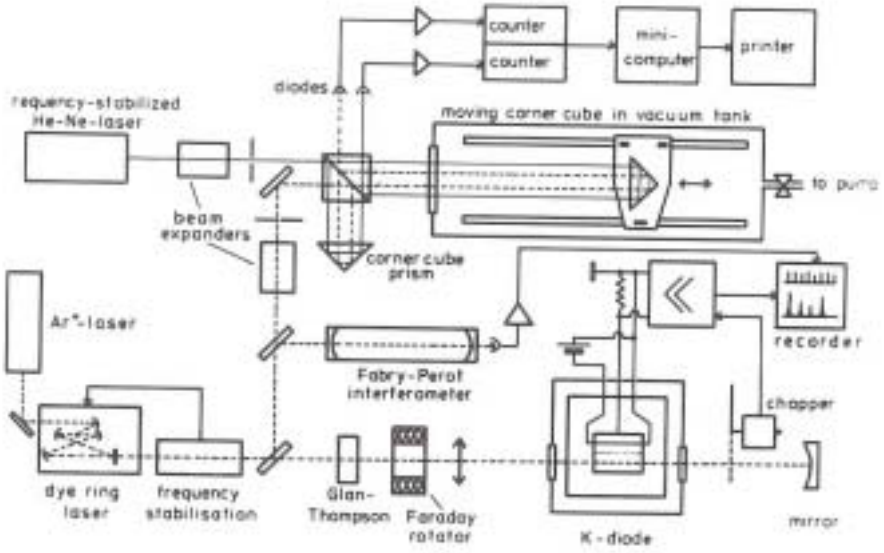

Fig. 42. High-precision evacuated optical wavemeter (from Ref. 44).

The direct frequency measurement technique in the visible and near-infrared consists of developing a beat signal between the unknown frequency and a high harmonic of a known frequency, which is referred ultimately to a basic time standard such as an atomic clock. Because of the high frequency ratio (of order 10^{14} Hz/10^{7} Hz = 10^{7}), several stages are needed. Figure 43 shows such a referencing scheme for the microwave-to-infrared step.[45] Several phase-locked klystron oscillators produce harmonics in the region of 10^{10} to 10^{11} Hz. Then a series of lasers, a formaldehyde laser, a methanol laser, a carbon dioxide laser, another carbon dioxide laser, and so on, extend the range the rest of the way. All beat frequencies are either measured or servo-locked to known values, so that the final optical frequency is absolutely known. As can be imagined, these comparison chains require a room full of apparatus. There are several such chains in existence:[46] at the National Physical Laboratory in England, at the National Research Council of Canada, at the National Bureau of Standards in Boulder, Colorado, USA, and in France, Germany, Japan, and the USSR. Figure 44 shows ratioing details of the NBS, NRC, and NPL chains. In addition, there are at least three infrared-to-visible chains in existence: at NBS, NRC, and the Institute for Semiconductor Physics in Novosibirsk, USSR. Figure 45 shows ratioing details of the infrared-to-visible chains.

C. Harmonic generation and frequency mixing

The heart of any frequency ratioing scheme must be a nonlinear mixing device, since if waves of two or more frequencies are combined in a linear device, no new Fourier components are generated. Various approaches, involving plasmas, electron tubes, nonlinear gases, vapors,

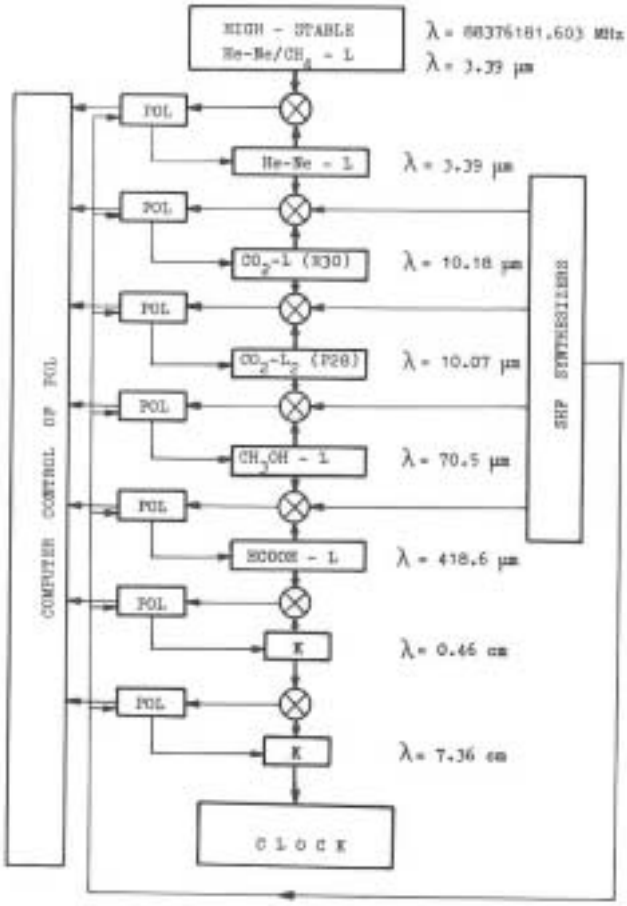

Fig. 43. Microwave-to-infrared frequency reference chain (from Ref. 45).

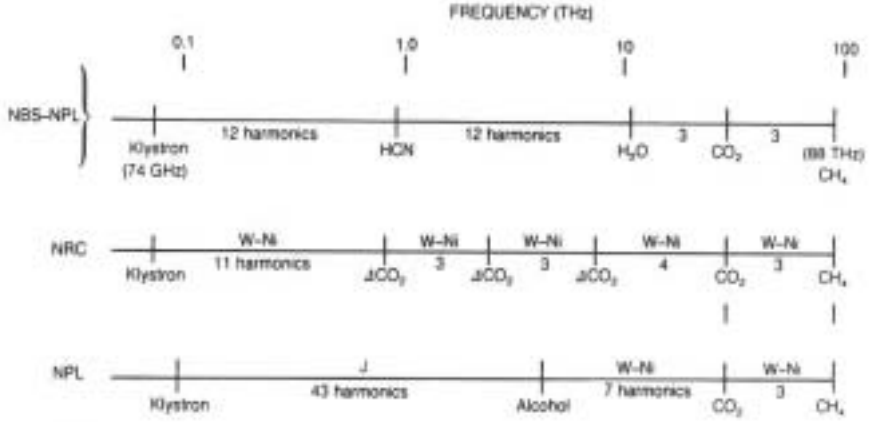

Fig. 44. Three microwave-to-infrared frequency ratioing schemes (from Ref. 46).

surfaces and interfaces, and point-contact diodes, have been used for nonlinear mixing in the radio-frequency and microwave regimes. The one that has been translated most successfully into the optical region is the tungsten-nickel point-contact diode, which is readily capable of mixing microwave and infrared frequencies, and two or more infrared

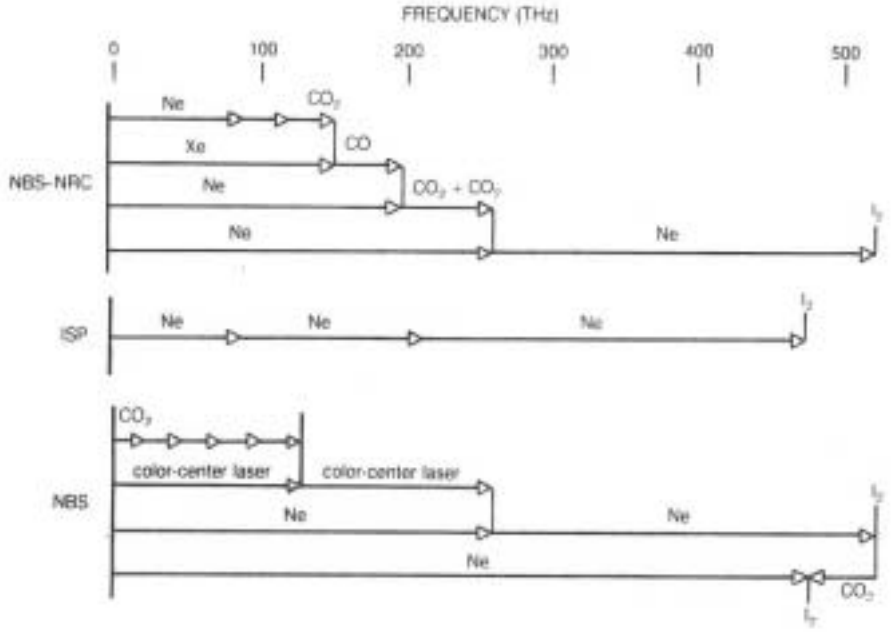

Fig. 45. Three infared-to-visible frequency ratioing schemes (from Ref. 46).

frequencies that are widely spaced. Figure 46 is a photograph of one of those devices.[46] It is made by etching a tungsten wire to a fine point of a few microns radius, and touching it delicately to a polished or vacuum-evaporated nickel surface. The nonlinearity comes from the electrical properties of the interface between the tungsten, the nickel, and whatever impurity film is on the surface; the details are not well understood.

The tungsten wire functions as a long-wire antenna to collect light energy for driving the diode and also for radiating combination frequencies the diode generates. Recently, about 10^{-7} W of radiated power at 500 GHz has been generated by one of these diodes when illuminated by two CO_2 laser lines whose frequencies $\nu \simeq 30{,}000$ GHz differed by that amount.[52] Efficient coupling requires that each input radiation field impinges upon the diode at an angle which is near the peak of a strong lobe of the antenna pattern for the frequency of that radiation field, and the efficient extraction of power has a similar requirement.

D. Noise in frequency multiplier chains

A difficulty with harmonic generation to relate high frequency signals to low frequency ones can be seen from the following argument. Consider a diode harmonic generator having an nth-order nonlinearity, so that

$$V_{out} = K(I_{in})^n . \qquad (27)$$

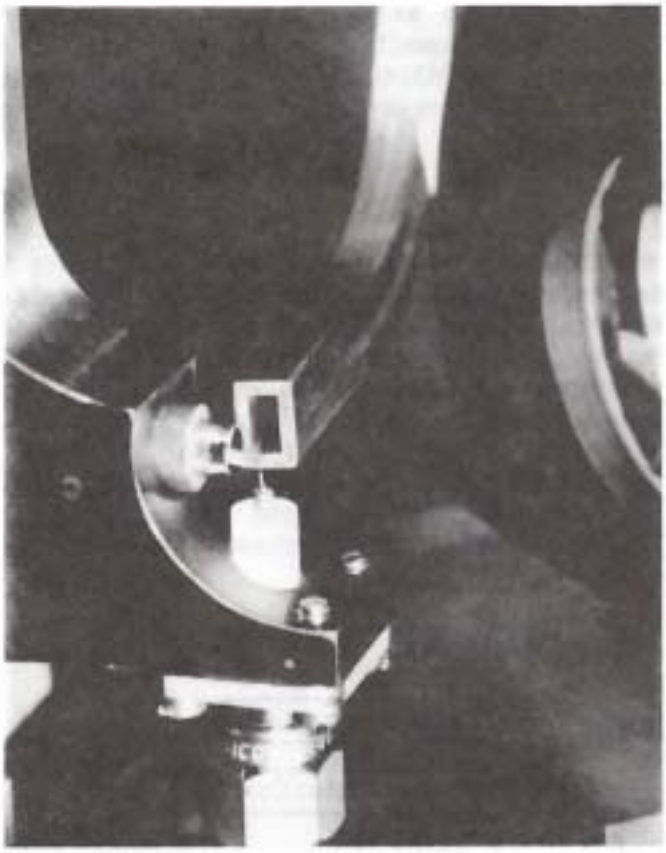

Fig. 46. Tungsten-nickel optical mixing diode (from Ref. 46).

Then if the input current is

$$I_{in} = (I_o/2)e^{i\omega t} + c.c. , \tag{28}$$

the output voltage is

$$V_{out} = K(I_o/2)^n [e^{in\omega t} + \text{cross terms} + c.c.] , \tag{29}$$

and contains a strong component at frequency $n\omega$. If the input includes sideband noise of relative amplitude ε and frequency offset δ, then

$$I_{in} = (I_o/2) [e^{i\omega t} + \varepsilon e^{i(\omega+\delta)t} + c.c.] , \tag{30}$$

and the output voltage is

$$V_{out} = K(I_o/2)^n [e^{in\omega t} + n\varepsilon e^{i(n\omega+\delta)t} + \ldots + \text{cross terms} + c.c.] . \tag{31}$$

And the harmonic generation process has increased the sideband noise intensity (= the square of the amplitude) by a factor of n^2 relative to the main frequency intensity. In practice the sideband noise in a high harmonic generated in this way from a low-frequency time standard may be much greater than that in the optical-frequency oscillation signal we wish to stabilize or calibrate. Thus in order to preserve the benefits of the latter's narrow bandwidth, we must filter the beat frequency

between the two, or limit the bandwidth of the stabilizing servoloop. Then it becomes necessary that each oscillator in the chain have independent high short-term frequency stability, since a narrow-bandwidth servoloop can only affect the long-term-averaged frequency of the oscillator it controls.

E. Ultimate source linewidth

There are many possible sources of noise in a physical laser; the main contributions are depicted schematically in Fig. 47. The theoretical minimum noise bandwidth is obtained when all noise sources except spontaneous emission are removed (assuming, as is the case at present, that no practical way of suppressing spontaneous emission has been found). Then, if the stimulated emission electric field in the active laser cavity mode is represented by a long phasor (vector rotating at the mean output frequency ω) of length $\bar{n} \gg 1$, where $\bar{n}$ is the mean number of photons in the mode, the spontaneous emission into the same mode is represented by a short random phasor which causes phase fluctuations of

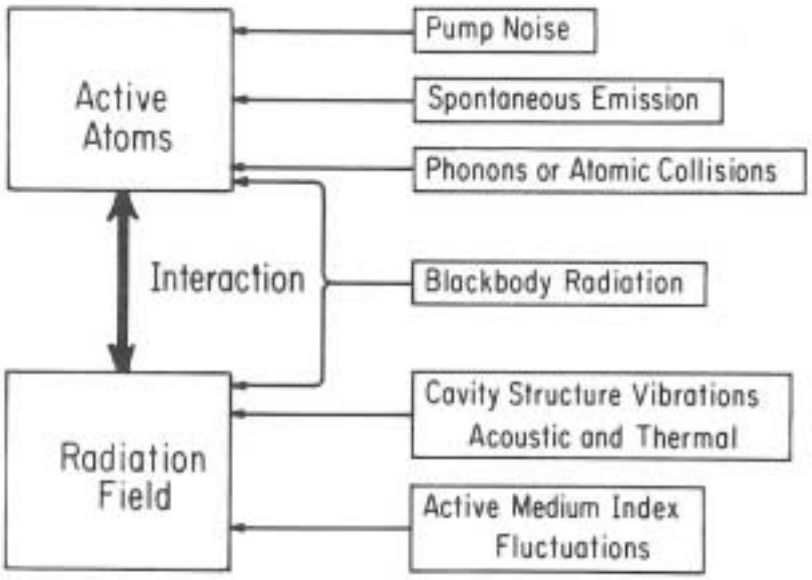

Fig. 47. Noise sources in a physical laser.

the resultant and hence broadens the laser spectrum. Well above threshold, the laser linewidth can be expressed as[47]

$$\Delta\nu_{laser} = \left[\frac{2\pi h\nu(\Delta\nu_{1/2})^2}{P_e}\right]\left[\frac{N_2}{N_2-(g_2/g_1)N_1}\right], \qquad (32)$$

where $h\nu$ is the photon energy, $\Delta\nu_{1/2}$ is the full width of the passive cavity resonance, P_e is the emitted power, and N_2,g_2 (N_1,g_1) are the population and the degeneracy factor of the upper (lower) laser level.

Evidently to obtain a narrow line we must make $\Delta\nu_{1/2}$ small and P_e large; thus the cavity Q should be high and the output coupling weak. It should be noted that P_e is the net rate of emission of energy by the laser medium, and does not become zero even if no power is coupled out, since there are internal losses, e.g., from the mirror absorptivity. The cavity resonance width can be further related to the losses: $\Delta\nu_{1/2} = (2\pi t_c)^{-1}$, where t_c is the cavity decay time; and t_c can be expressed as $2\ell/c$ [the passive cavity round-trip time] divided by [the fractional energy loss per round trip]. Typical numerical values are given in Table IV.

TABLE IV. Estimates of ultimate resolution of two common laser oscillators.

Quantity	He-Ne, 6328 Å	CO_2, 10 μm
ν	4.74×10^{14} Hz	3×10^{13} Hz
ℓ	100 cm	150 cm
round trip loss	2%	10%
$\Delta\nu_{1/2}$	4.8×10^{5} Hz	1.6×10^{6} Hz
P_e	1 mW	3 W
N_2/N_1	>> 1	>> 1
$\Delta\nu_{laser}$	4.5×10^{-4} Hz	1.1×10^{-7} Hz
$Q_\nu \equiv \nu/\Delta\nu_{laser}$	1.0×10^{18}	2.8×10^{20}

It is likely that $\Delta\nu_{laser}$ as calculated from Eq. (32) could be reduced even further by careful optimization of laser parameters. Thus it can be seen that extremely high spectroscopic resolution is available in principle using common laser types. In practice, however, the many effects in Fig. 47 other than spontaneous emission will require careful attention as well.

F. Ultimate sample linewidth

Figure 48 shows the quality factor Q_ν for several high-Q spectroscopic situations.[49] Some of these are theoretical limits; for example, the ^{57}Fe value is for the Mossbauer transition in the nucleus, spontaneously broadened . Others, particularly below the dotted line, are practical values for mature experimental situations. The criterion for high theoretical Q_ν is a high transition frequency combined with a low spontaneous decay rate. The rapid decrease of the latter with decreasing frequency makes trapped homonuclear diatomic molecular ions

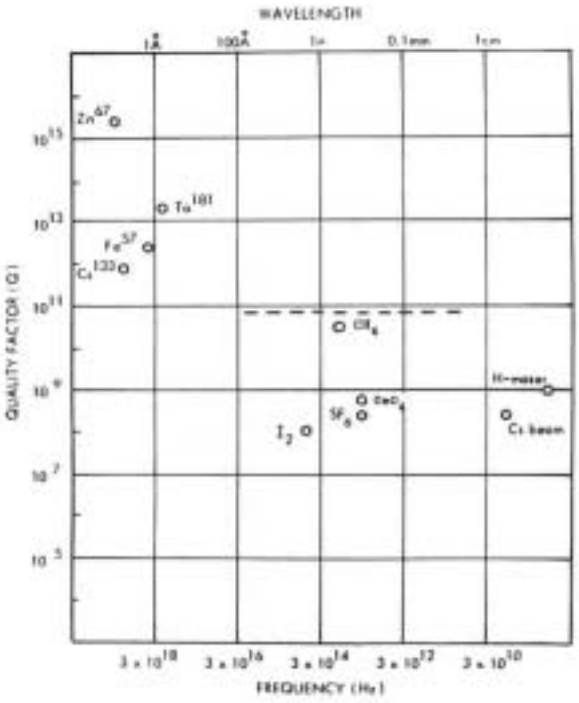

Fig. 48. Some exceptionally high-Q_ν spectroscopic resonances (from Ref. 49). Even higher-Q_ν cases exist in homonuclear molecular ions (see text).

attractive candidates in addition to those shown; the Q_ν values for vibrational and rotational transitions in light ions such as H_2^+ are on the order of 10^{18} to 10^{20}. The excited vibrational and rotational states decay (via electric quadrupole radiation) in times on the order of minutes to days; thus their high Q_ν's are in principle experimentally accessible, in contrast to those of hyperfine transitions in ground-state atoms: Although the theoretical Q_ν values of the latter may be many orders of magnitude larger than any others yet mentioned, the undisturbed observation time required to utilize them may well exceed the lifetime of the apparatus or its operator.

XI. SOME PROSPECTIVE APPLICATIONS OF ULTRAHIGH-RESOLUTION SPECTROSCOPY

It is simplest to summarize these largely speculative possibilities in a table, and leave the details to the imagination of the reader, since that is always the final ingredient in spectroscopic progress.

TABLE V.

Phenomenon	Resolution needed to detect
Isomeric shift in an atomic frequency due to nuclear excitation	$10^{8} - 10^{10}$
Weak interaction shift in chiral molecules	$10^{14} - 10^{15}$
Long-range interaction between molecular nuclei	$10^{10} - 10^{14}$
New limit on time variation of fine structure constant α via time variation of fine/gross structure or hyperfine/fine structure transition frequency ratio	$10^{13} - 10^{16}$
Gravitational effects on trapped ion energy levels	$10^{11} - 10^{13}$
Excitation mass-energy shift of a trapped particle motional resonance	$10^{8} - 10^{9}$

REFERENCES

1. G. W. Series, The Spectrum of Atomic Hydrogen (Oxford University Press, London, 1957).
2. H. A. Bethe and E. E. Salpeter, Quantum Mechanics of One- and Two-Electron Atoms (Springer-Verlag, Berlin, 1957).
3. T. W. Hänsch, A. L. Schawlow, and G. W. Series, Scientific American 240, 94 (1979).
4. N. Bohr, Philos. Mag. 26, 1 (1913).
5. P. A. M. Dirac, Proc. R. Soc. London A 117, 610 (1928).
6. R. P. Feynman, Phys. Rev. 76, 769 (1949).
7. J. Schwinger, Phys. Rev. 74, 1439 (1948); 75, 651 (1949).

8. S. Tomonaga, Prog. Theor. Phys. (Kyoto) 1, 27 (1946); Phys. Rev. 74, 224 (1948).

9. T. F. Gallagher and W. E. Cooke, Phys. Rev. Lett. 42, 835 (1979); W. E. Cooke and T. F. Gallagher, Phys. Rev. A 21, 588 (1980).

10. J. W. Farley and W. H. Wing, Phys. Rev. A 23, 2397 (1981).

11. W. H. Wing, G. A. Ruff, W. E. Lamb, Jr., and J. J. Spezeski, Phys. Rev. Lett. 36, 1488 (1976).

12. W. H. Wing, in Laser Spectroscopy III, J. L. Hall and J. L. Carlsten, Eds. (Springer-Verlag, New York, Heidelberg, 1977), pp. 69-75.

13. W. H. Wing, in 1978 McGraw-Hill Yearbook of Science and Technology (McGraw-Hill, New York, 1978), pp. 266-269.

14. D. E. Tolliver, G. A. Kyrala, and W. H. Wing, Phys. Rev. Lett. 43, 1719 (1979).

15. J.-T. Shy, J. W. Farley, W. E. Lamb, Jr., and W. H. Wing, Phys. Rev. Lett. 45, 535 (1980).

16. J.-T. Shy, J. W. Farley, and W. H. Wing, Phys. Rev. A 24, 1146 (1981).

17. W. H. Wing, IEEE Trans. Nucl. Sci. 28, 1178 (1981).

18. W. E. Lamb, Jr., Phys. Rev. 134, 1429 (1964).

19. R. A. McFarlane, W. R. Bennett, and W. E. Lamb, Appl. Phys. Lett. 2, 189 (1963).

20. T. W. Hänsch, I. S. Shahlin, and A. L. Schawlow, Phys. Rev. Lett. 27, 707 (1971).

21. W. E. Lamb, Jr. and R. C. Retherford, Phys. Rev. 72, 241 (1947); W. E. Lamb, Jr. and R. C. Retherford, Phys. Rev. 79, 549 (1950); ibid, Phys. Rev. 81, 222 (1951); ibid, Phys. Rev. 85, 259 (1952); S. Triebwasser, E. S. Dayhoff, and W. E. Lamb, Jr., Phys. Rev. 89, 98 (1953); E. S Dayhoff, S. Triebwasser, and W. E. Lamb, Jr., Phys. Rev. 89, 106 (1953).

22. M. S. Sorem, M. D. Levenson, and A. L. Schawlow, Phys. Lett. 37A, 33 (1971).

23. C. Weiman and T. W. Hänsch, Phys. Rev. Lett. 36, 1170 (1976).

24. T. Wik, W. R. Bennett, and W. Lichten, Phys. Rev. Lett. 40, 1080 (1978); S. R. Amin, C. D. Caldwell, and W. Lichten, Phys. Rev. Lett. 47, 1236 (1981).

25. B. Cagnac, G. Grynberg, and F. Biraben, J. Phys. (Paris) 34, 56 (1973), and Phys. Rev. Lett. 32, 643 (1974); M. D. Levenson and N. Bloembergen, Phys. Rev. Lett. 32, 645 (1974); T. W. Hänsch, K. C.

Harvey, G. Meisel, and A. L. Schawlow, Opt. Commun. 11, 50 (1974).

26. G. Grynberg, F. Biraben, M. Bassini, and B. Cagnac, Phys. Rev. Lett. 37, 283 (1976).

27. T. W. Hänsch, S. A. Lee, R. Wallenstein, and C. Weiman, Phys. Rev. Lett. 34, 307 (1975).

28. I. I. Rabi, Phys. Rev. 51, 652 (1937).

29. See N. F. Ramsey, Molecular Beams (Clarendon Press, Oxford, U.K., 1956), Ch. V.

30. J. E. Thomas, P. R. Hemmer, S. Ezekiel, C. C. Leiby, Jr., R. H. Picard, and C. R. Willis, Phys. Rev. Lett. 48, 867 (1982).

31. W. E. Lamb, Jr., Phys. Rev. 51, 187 (1937).

32. Duane's analysis is given by W. Heisenberg, in The Physical Principles of the Quantum Theory, University of Chicago Lectures (Dover Publications, 1930), pp. 77-78.

33. H. Frauenfelder, The Mössbauer Effect (Benjamin, New York, 1962).

34. R. V. Pound and G. A. Rebka, Jr., Phys. Rev. Lett. 4, 337 (1960).

35. R. H. Dicke, Phys. Rev. 89, 472 (1953).

36. H. M. Goldenberg, D. Kleppner, and N. F. Ramsey, Phys. Rev. Lett. 5, 361 (1960).

37. D. J. Wineland, W. M. Itano, and R. S. Van Dyck, Jr., in Advances in Atomic and Molecular Physics 19, (1982) (to be published).

38. W. Neuhauser, M. Hohenstatt, P. E. Toschek, and H. Dehmelt, in Spectral Line Shapes, B. Wende, Ed. (W. de Gruyter & Co., Berlin, 1981), pp. 1045-1070.

39. R. E. Drullinger, D. J. Wineland, and J. C. Bergquist, Appl. Phys. 22, 365 (1980).

40. D. J. Wineland and W. M. Itano, Phys. Lett. 82A, 75 (1981); D. J. Wineland, J. C. Bergquist, R. E. Drullinger, H. Hemmati, W. M. Itano, and F. L. Walls, J. de Physique 42, C8-307 (1981).

41. W. Neuhauser, M. Hohenstatt, P. E. Toschek, and H. Dehmelt, Phys. Rev. A 22, 1137 (1980).

42. I am grateful to D. E. Pritchard for pointing out that the internal-energy-dependence of the atomic inertial mass may be measurable using SQUID technology.

43. A. G. Vaidyanathan, W. P. Spencer, and D. Kleppner, Phys. Rev. Lett. 47, 1592 (1981).

44. C.-J. Lorenzen, K. Niemax, and L. R. Pendrill, Opt. Commun. 39, 6 (1981).

45. V. P. Chebotayev, V. G. Goldort, V. M. Klementyev, M. V. Nikitin, B. A. Timchenko, and V. F. Zakharyash, Appl. Phys. B 29, 63 (1982).

46. K. M. Baird, Physics Today 36, 52 (January 1983).

47. A. Yariv, Quantum Electronics, 2nd ed. (John Wiley & Sons, New York, 1975), p. 303.

48. F. M. Pipkin and R. C. Ritter, Science 219, 913 (1983).

49. V. S. Letokhov and V. P. Chebotaev, Nonlinear Laser Spectroscopy (Springer-Verlag, Berlin, 1977).

50. H. Hellwig, K. Evenson, and D. J. Wineland, Physics Today 31, 23 (1978).

51. R. Blatt, H. Schnatz, and G. Werth, Phys. Rev. Lett. 48, 1601 (1982).

52. K. Evenson, personal communication.

53. E. Bergstrand, in Handbuch der Physik, S. Flügge, Ed. (Springer-Verlag, Berlin, 1956), V. 24, p. 1.

54. R. T. Birge, Nuovo Cimento 6, 39 (1957).

55. E. R. Cohen and J. W. M. Dumond, Rev. Mod. Phys. 37, 537 (1965).